

Spin Singlet Mott States and Evidence For Spin Singlet Quantum Condensates of Spin-One Bosons in Lattices

Fei Zhou^{†,††} and Michiel Snoek[†]

ITP, Utrecht University, Leuvenlaan 4, 3584 CE Utrecht, The Netherlands[†]

Department of Physics and Astronomy, University of British Columbia,

6224 Agriculture Road, Vancouver, B.C. V6T 1Z1, Canada^{††}*

(October 24, 2018)

We have investigated spin singlet Mott states of spin-one bosons with antiferromagnetic interactions. These spin singlet states do not break rotational symmetry and exhibit remarkably different macroscopic properties compared with nematic Mott states of spin-one bosons. We demonstrate that the dynamics of spin singlet Mott states is fully characterized by even- or odd-class quantum dimer models. The difference between spin singlet Mott states for even and odd numbers of atoms per site can be attributed to a selection rule in the low energy sectors of on-site Hilbert spaces; alternatively, it can also be attributed to an effect of Berry's phases on bosonic Mott states.

We also discuss evidence for spin singlet quantum condensate of spin-one atoms. Our main finding is that in a projected spin singlet Hilbert space, the low energy physics of spin-one bosons is equivalent to that of a Bose-Hubbard model for *spinless* bosons interacting via Ising gauge fields. The other major finding is spin-charge separation in some one-dimensional Mott states. We propose charge- e spin singlet superfluid for an odd number of atoms per lattice site and charge- $2e$ spin singlet superfluid for an even number of atoms per lattice site in one-dimensional lattices. All discussions in this article are limited to integer numbers of bosons per site.

PACS number: 03.75.Mn, 05.30.Jp, 75.10.Jm

I. INTRODUCTION

Spin correlated condensates of spin-one atoms have attracted considerable interest since 1998 [1,2]. Two-body scattering between atoms leads to either antiferromagnetic (polar) or ferromagnetic condensates [3–5]. For spin-one bosons with antiferromagnetic interactions, the condensates break both the rotational symmetry and the $U(1)$ symmetry associated with the phases of the condensates. There are two branches of spin-wave excitations and one gapless phason mode. For a condensate of a finite size, the exact ground state however is a spin singlet (assuming the total number of atoms is even) which on the other hand is extremely sensitive to external perturbations [5,6]. In rotating traps, two-body scatterings furthermore result in spin correlated fractional quantum Hall states [7,8].

In lattices where the hopping is small, bosonic particles can be localized because of repulsive interactions and ground states in this limit are Mott insulators [9]. Mott-insulating states of cold atoms have been recently observed in optical lattices [10]. Spin correlated Mott-insulating states in high dimensional optical lattices have also been investigated theoretically and reported in [11]. Both nematic Mott insulators which break the rotational symmetry and spin singlet Mott insulating states were

found for high dimensional lattices in certain parameter regime. Other spin correlated states which break both translational and rotational symmetries were proposed in [12]. Effects of spin correlations on Mott insulator-superfluid transitions were suggested and remain to be fully understood [13]. Very recently, detailed analyses of microscopic wave functions and phase transitions between spin singlet Mott insulators and nematic ones have been carried out [14,15]. In the context of antiferromagnets, the issue of spin nematic states was raised and addressed previously [16–18].

To distinguish different correlated states of spin-one bosons in a lattice, it is useful to introduce the following order parameters in terms of creation and annihilation operators ψ_α^\dagger , ψ_α respectively ($\alpha = x, y, z$);

$$\begin{aligned}\mathcal{O}_\alpha^1 &= \langle \psi_{k\alpha} \rangle, \\ \mathcal{O}_{\alpha\beta}^2 &= \langle \psi_{k\alpha}^\dagger \psi_{k\beta} \rangle - \frac{1}{3} \delta_{\alpha\beta} \langle \psi_{k\gamma}^\dagger \psi_{k\gamma} \rangle.\end{aligned}\quad (1)$$

In Eq.1, we have employed the following creation operators

$$\begin{aligned}\psi_x^\dagger &= \frac{1}{\sqrt{2}}(\psi_{-1}^\dagger - \psi_1^\dagger), \\ \psi_y^\dagger &= \frac{i}{\sqrt{2}}(\psi_1^\dagger + \psi_{-1}^\dagger), \\ \psi_z^\dagger &= \psi_0^\dagger.\end{aligned}\quad (2)$$

*Permanent address

where $\psi_{m_F}^\dagger$, $m_F = \pm 1, 0$, are creation operators of spin-one bosons with $S_z = m_F$.

In terms of these order parameters, polar condensates (pBEC), nematic Mott insulators (NMI) and spin singlet Mott insulating states (SSMI) have the following properties

$$\begin{aligned} \text{pBEC} : \mathcal{O}_\alpha^1 &\neq 0, \mathcal{O}_{\alpha\beta}^2 \neq 0; \\ \text{NMI} : \mathcal{O}_\alpha^1 &= 0, \mathcal{O}_{\alpha\beta}^2 \neq 0; \\ \text{SSMI} : \mathcal{O}_\alpha^1 &= 0, \mathcal{O}_{\alpha\beta}^2 = 0. \end{aligned} \quad (3)$$

Finally, for all states of cold atoms with antiferromagnetic interactions which interest us in this paper, the expectation value of spin operators is zero

$$\langle \mathbf{S} \rangle = 0, \mathbf{S}^\alpha = -i\epsilon^{\alpha\beta\gamma} \psi_\beta^\dagger \psi_\gamma; \alpha, \beta, \gamma = x, y, z. \quad (4)$$

Spin correlations in Mott-insulating states also depend on the even-odd parity of numbers of atoms per site. While spin correlated Mott states for even numbers of atoms per site have been studied and understood, states for odd numbers of atoms per site remain to be fully understood. In one-dimensional optical lattices, it was argued that spin singlet Mott states for an odd number of atoms per site should be dimerized-valence-bond crystal (DVBC) states [19,14]. These DVBC states are characterized by the following nontrivial spin correlations:

$$\langle \mathbf{S}_i \cdot \mathbf{S}_{i+1} \mathbf{S}_{i+2k} \cdot \mathbf{S}_{i+2k+1} \rangle \neq 0 \quad (5)$$

when k approaches ∞ (for either all even i or all odd i only). Later, we present more evidence for the existence of DVBC Mott states; certain aspects of long wave length behaviors of DVBCs found for spin-one bosons are similar to those of DVBC states in $S = 1$ spin chains [20–25].

Valence-bond crystal states and more generally spin-Peirls states have been proposed in various models for strongly correlated electrons. Possible spin-Peirls states in 2D antiferromagnets (disordered) due to Berry's phases carried by hedgehogs were pointed out in [26]. In $SU(N)$ -antiferromagnet models or their effective models, valence-bond crystal phases were discovered in various limits [27–29]. Most recently, valence-bond crystals in strongly-correlated systems due to Berry's phases in Ising gauge fields were addressed [30,31]. In quantum dimer models, crystal phases have been anticipated in [32], and were reviewed in a recent paper [33].

Condensates for spin-one bosons with antiferromagnetic interactions in lattices also have fascinating properties; most of arguments in the weakly interacting case can be carried out parallel to those developed for the continuous limit. Particularly, ground state wave functions should possess Ising gauge symmetries; and condensates support interesting half-vortex-type topological excitations in addition to usual integer vortices [34]. Furthermore, the local spin dynamics is described by a

nonlinear sigma model; for an individual condensate in a zero-mode approximation, a constrained $O(3)$ -quantum-rotor model can be introduced to characterize the spin dynamics. Due to spin-phase separation there are a variety of novel spin correlated "condensates"; particularly, we will argue that there should be spin singlet quantum condensates (SSQCs), in addition to usual polar condensates.

Early indication for spin singlet quantum condensates, or rotationally invariant condensates came from the analysis of renormalization-group equations. The phenomenon of spin-phase separation implies that orders be established in either phase, or spin sector but not necessary in both. Particularly, there exist rotationally invariant superfluid states [34]. In fact, the failure of order parameters (when treated as quantum operators) to commute with the Hamiltonian eventually leads to these fascinating many-body condensates of spin-one bosons. From this point of view, a polar condensate is a "classical" one, of which order parameter operators can be approximated as classical variables.

The second relevant observation on spin singlet condensates was made in [11]. There, the authors consider a limit where two-body repulsive interactions in ferromagnetic channels are much stronger than in singlet channels. In this limit, atoms form singlet pairs and condense; the resultant state is a condensate of spin singlet pairs. The solution in this limit is consistent with general arguments based on renormalization-group equations; furthermore, it indicates a microscopic realization of rotationally invariant condensates suggested by renormalization-group equations. In [35], the authors further analyzed a few other spin singlet states, some of which break time reversal symmetry and have fascinating edge properties.

The most recent indication of SSQCs is the phenomenon of fractionalization in some Mott states. Consider each cold atom as a particle with spin $S = 1$ and "charge" $Q = e$. The spin-"charge" separation in Mott insulating states for spin-one bosons with antiferromagnetic interactions implies fractionalization of cold atoms in optical lattices; it also offers some insight into microscopic wavefunctions of fractionalized condensates. The ground state of interacting spin-one bosons in the strong coupling limit can be a DVBC; and this state supports either spinful but chargeless quasi-particles or charged but spinless quasi-particles in one-dimensional limit [19]. The low-energy sector of the Hilbert space can thus be divided into two subsectors of spin and charge. All the low lying excitations live in one of these two sectors. Therefore, each atom injected into a lattice naturally fractionalizes into spinless *charge- e* ($Q = 1, S = 0$) excitations and chargeless but spinful ($Q = 0, S = 1$) excitations. Theoretically, the novel SSQCs appear naturally as a result of condensation of spinless charge- e bosons. In this article, we substantiate those proposals made in [19]; particularly we demonstrate the microscopic structure of

possible charge-e spin singlet condensates [36].

The fractionalization of cold atoms to be discussed in this article is an analogy of spin-charge separation proposed in strongly interacting electron systems. For strongly-correlated electrons in cuprates, the concept of spin-charge separation was emphasised in [37]; the phenomenon of spin-charge separation in doped antiferromagnets was studied afterwards in terms of effective compact gauge fields [38,39]. Many attempts have since then been made to understand the fractionalization of electrons in cuprates [27,32,40–46]. In some subsequent works, fractionalization in quantum spin liquids was investigated in the context of effective Ising gauge theories [28,29,47]. Most recent efforts on this subject can be found in [48,30,31,50,49,33,51]; especially, superconducting states of "chargons" (charge-e objects) have been proposed in [30,51]. Some general discussions on spin-charge separation can be found in a remarkable book [52].

It is worth pointing out that from the point of view of fractionalized atoms, in some Mott insulating states only a fraction of each spin-one boson appears to be "localized"; these states display rather interesting internal coherence as a result of "partial condensation". For instance, nematic Mott insulating states can be effectively considered as condensates of fractionalized spinful but chargeless particles or spin-one *spinons*. In appendix C, we examine spin correlated Mott states from this point of view. Our discussions will be limited to cases of integer numbers of bosons per site; condensates for non-integer numbers of bosons per site will be addressed in a future paper.

In this article, we develop a general approach for the studies of spin singlet states. First, we demonstrate that all SSMIs can be fully characterized by even- and odd-class quantum dimer models. In the second part of the article, we pursue the idea of SSQCs of spin-one bosons in lattices; particularly, we provide various evidence for these unconventional spin correlated condensates. In SSQCs, condensation takes place only in the charge sector of the Hilbert space. SSQCs therefore exhibit distinct long-range order. It is possible to distinguish them from pBECs in experiments because of remarkably distinct macroscopic properties of SSQCs.

In section II, we summarize results on spin-correlated Mott states of spin-one bosons in lattices and present microscopic wavefunctions for some of the states. In section III, we investigate spin singlet Mott states for odd numbers of atoms per site in one-dimensional lattices in the extremely small hopping limit. In section IV, we discuss excitations in spin singlet Mott states; we demonstrate the fractionalization of spin-one atoms in DVBCs in one-dimensional lattices. In section V, we present a qualitative picture of SSQCs using a projected spin singlet Hilbert space; we argue that spin correlations strongly suppress one-particle hopping in an SSMI for an even number of bosons per site. In section VI, we introduce

a fractionalized representation for interacting spin-one bosons in a lattice. In section VII, we briefly present results on SSMIs and SSQCs in high dimensional lattices. In section VIII, we revisit low-dimensional SSMIs using an approach based on quantum dimer models; particularly, we generalize the results on one-dimensional lattices in section III to the entire Mott phase (one-dimensional). In section IX, we discuss SSQCs in one-dimensional lattices. In section X, we address the issue of the possible role of Berry's phases in one-dimensional lattices.

It was demonstrated and emphasized in a few occasions that the problem of interacting spin-one bosons can be mapped into a constrained quantum rotor model (CQR) [34,11]. Technically, this allows one to acquire certain valuable intuition about many strongly-correlated states of spin-one bosons using the knowledge about the renormalization-group equations and topological field theories. The mapping is therefore a powerful device to study properties of spin-one bosons in optical lattices. The resultant CQR model will be our starting point for the studies of spin-one bosons in lattices.

II. SPIN CORRELATED MOTT STATES: A SHORT REVIEW

For spin-one bosons with antiferromagnetic interactions in (optical) lattices, the effective Hamiltonian can be conveniently expressed as

$$\mathcal{H}_{lat.} = -\tilde{t} \sum_{\langle kl \rangle} (\psi_{k\alpha}^\dagger \psi_{l\alpha} + h.c.) + \sum_k \frac{\mathbf{S}_k^2}{2I} + \frac{\hat{\rho}_k^2}{2C} - \hat{\rho}_k \mu \quad (6)$$

where the sum $\langle kl \rangle$ is carried out over neighboring sites k and l ; in this section, we are only interested in high dimensional bipartite lattices.

In Eq.6, $E_s = 1/2I$ and $E_c = 1/2C$ are two energy gaps in the excitation spectra of an individual condensate at each site. \tilde{t} is the hopping integral; μ is the chemical potential. $N_0 (\gg 1)$ will be the number of bosons per site. The dynamics is defined by the following commutation relations,

$$[\mathbf{S}_k^\alpha, \psi_{l\beta}] = i\epsilon^{\alpha\beta\gamma} \delta_{kl} \psi_{k\gamma}, [\hat{\rho}_k, \psi_{l\alpha}^\dagger] = \delta_{kl} \delta_{\alpha\beta} \psi_{l\beta}^\dagger \quad (7)$$

where

$$\mathbf{S}_k^\alpha = -i\epsilon^{\alpha\beta\gamma} \psi_{k\beta}^\dagger \psi_{k\gamma}, \rho_k = \psi_{k\alpha}^\dagger \psi_{k\alpha} \quad (8)$$

are the spin and "charge" operators for spin-one bosons, $\alpha(\beta, \gamma) = x, y, z$. And

$$[\mathbf{S}_k^\alpha, \mathbf{S}_{k'}^\beta] = i\epsilon^{\alpha\beta\gamma} \delta_{k,k'} \mathbf{S}_k^\gamma, [\mathbf{S}_k^\alpha, \hat{\rho}_{k'}] = 0 \\ [\mathbf{S}_k^\alpha, \psi_{k'\beta}^\dagger \psi_{k'\beta}] = [\mathbf{S}_k^\alpha, \psi_{k'\beta} \psi_{k'\beta}^\dagger] = 0 \quad (9)$$

In addition,

$$\mathbf{S}_k^2 = \hat{\rho}_k(\hat{\rho}_k + 1) - \psi_{k\alpha}^\dagger \psi_{k\alpha}^\dagger \psi_{k\beta} \psi_{k\beta} \quad (10)$$

where $\psi_\alpha^\dagger \psi_\alpha^\dagger$ is a singlet pair creation operator. Following this identity, $\mathbf{S}_k^2 = S_k(S_k + 1)$ and $S_k = 0, 2, 4, \dots, 2n$, if $\rho_k = 2n$; otherwise $S_k = 1, 3, 5, \dots, 2n + 1$ if $\rho_k = 2n + 1$. For spin-one bosons with antiferromagnetic interactions, the ground state for an isolated site with $\rho_k = 2n$ atoms is a spin singlet and for $\rho_k = 2n + 1$ is a spin triplet [5].

Therefore at low energies, the Hilbert space of the Hamiltonian is subject to a constraint that the sum of the number of particles ρ_k and the total spin S_k , has to be an even number so that the many-boson wave function is symmetric under interchange of two spin-one particles. Say it differently, the Hilbert space displays the following selection rule

$$(-1)^{S_k + \rho_k} = 1 (S_k \leq \rho_k). \quad (11)$$

This **selection rule** plays an extremely important role in both symmetry breaking states and spin singlet Mott insulating states [11,14,15,19,34].

In optical lattices, the hopping \tilde{t} can be varied continuously as a function of laser intensity; \tilde{t} decreases as the laser intensity increases. $E_{s,c}$ on the other hand depend on the scattering lengths a_F , $F = 0, 2$

$$E_s = \frac{4\pi\rho_0(a_2 - a_0)}{3MN_0}, E_c = \frac{4\pi\rho_0(2a_2 + a_0)}{3MN_0}. \quad (12)$$

We will focus on the case when E_s is much less than E_c . As laser intensities are varied, we then have at least three different situations;

$$\begin{aligned} \text{i)} & t(V_{\text{opt}}) \gg E_c \gg E_s; \\ \text{ii)} & E_c \gg t(V_{\text{opt}}) \gg \sqrt{E_c E_s}; \\ \text{iii)} & E_c \gg \sqrt{E_c E_s} \gg t(V_{\text{opt}}). \end{aligned} \quad (13)$$

In Eq.13, $t = N_0 \tilde{t}$ is the effective hopping matrix element including a standard bosonic factor N_0 . The wave functions of spin correlated states we are interested in, can be conveniently expressed in a coherent state representation

$$|\mathbf{n}, \chi\rangle = \frac{1}{\sqrt{2\delta N}} \sum_{m=N_0-\delta N}^{N_0+\delta N} \exp(-im\chi) \frac{(\chi_\alpha^\dagger \mathbf{n}_\alpha)^m}{\sqrt{2(m-1)!}} |0\rangle, \quad (14)$$

with $\delta N \ll N_0$.

So at each site, one introduces two "collective" coordinates \mathbf{n}_k and $e^{i\chi_k}$, two unit vectors on a two-sphere S^2 and a unit circle S^1 which characterize the orientation of $O(3)$ and $O(2)$ quantum rotors respectively. Following Eqs.6-11, the Hamiltonian \mathcal{H}_{lat} . ($N_0, \delta N \gg 1$) in this representation can be expressed as \mathcal{H}_{CQR} of a constrained quantum rotor (CQR) model

$$\begin{aligned} \mathcal{H}_{\text{CQR}} = & -t \sum_{\langle kl \rangle} \mathbf{n}_k \cdot \mathbf{n}_l \cos(\chi_k - \chi_l) \\ & + \sum_k E_s \mathbf{S}_k^2 + E_c \rho_k^2 - \rho_k \mu. \end{aligned} \quad (15)$$

And

$$\begin{aligned} [\mathbf{S}_{k'}^\alpha, \mathbf{n}_k^\beta] &= -i\epsilon^{\alpha\beta\gamma} \delta_{k,k'} \mathbf{n}_k^\gamma, \mathbf{S}_k^\alpha = i\epsilon^{\alpha\beta\gamma} \mathbf{n}_k^\beta \frac{\partial}{\partial \mathbf{n}_k^\gamma}; \\ [\rho_{k'}, \chi_k] &= i\hbar \delta_{kk'}, \rho_k = i\hbar \frac{\partial}{\partial \chi_k}. \end{aligned} \quad (16)$$

As the orientation of the $O(3)$ -rotor at site k is specified as \mathbf{n}_k , the total spin at each site is defined as the angular momentum of this rotor, following Eq.15. The phase χ_k further defines the orientation of an $O(2)$ -rotor; the number operator corresponds to its angular momentum. The sum of S_k and ρ_k again is subject to the constraint in Eq.11. The Hamiltonian \mathcal{H}_{CQR} is locally invariant under a simultaneous inversion of \mathbf{n}_k and $\exp(i\chi_k)$. Introducing operators:

$$\begin{aligned} \hat{O}_k^x \Psi(\dots, \chi_k, \dots) &= \Psi(\dots, \pi + \chi_k, \dots) \\ \hat{O}_k^n \Psi(\dots, \mathbf{n}_k, \dots) &= \Psi(\dots, -\mathbf{n}_k, \dots) \end{aligned}$$

this invariance can be expressed as:

$$(\hat{O}_k^x \hat{O}_k^n)^{-1} \mathcal{H}_{\text{CQR}} \hat{O}_k^x \hat{O}_k^n = \mathcal{H}_{\text{CQR}}. \quad (17)$$

In the limit i), according to Eq.15, a usual polar condensate is established. A "mean field" polar condensate in this representation is

$$\Psi_{\text{pBEC}}(\{\mathbf{n}_k\}, \{\chi_k\}) \propto \prod_k \delta((\mathbf{n}_k \cdot \mathbf{n}_0) e^{i(\chi_k - \chi_0)} - 1) \quad (18)$$

where all directors \mathbf{n}_k point in the direction of \mathbf{n}_0 and all χ_k are "locked" at the same value of χ_0 . The wave function in Eq.18 explicitly exhibits the local Ising gauge symmetry emphasised in [34], i.e.

$$\hat{O}_k^n \hat{O}_k^x \Psi_{\text{pBEC}} = \Psi_{\text{pBEC}}. \quad (19)$$

Microscopically,

$$\Psi_{\text{pBEC}} \propto \frac{(\chi_{Q=0,\alpha}^\dagger \mathbf{n}_{0\alpha} \exp(i\chi_0))^{N_0 \times V_T}}{\sqrt{(N_0 \times V_T)!}} |0\rangle \quad (20)$$

represents a condensate at a state with zero crystal momentum $Q = 0$, along axis \mathbf{n}_0 ; $\chi_{Q\alpha}^\dagger = \frac{1}{\sqrt{V_T}} \sum \exp(i\mathbf{k} \cdot \mathbf{Q}) \chi_{k\alpha}^\dagger$, here V_T is the number of sites in a lattice.

In the limits of ii) and iii), particles are localized at each site and there are N_0 atoms per site. The wavefunction can be factorized into

$$\Psi(\{\mathbf{n}_k\}, \{\chi_k\}) = \Psi_{N_0}(\{\mathbf{n}_k\}) \otimes \prod_k \frac{1}{\sqrt{2\pi}} \exp(iN_0 \chi_k) \quad (21)$$

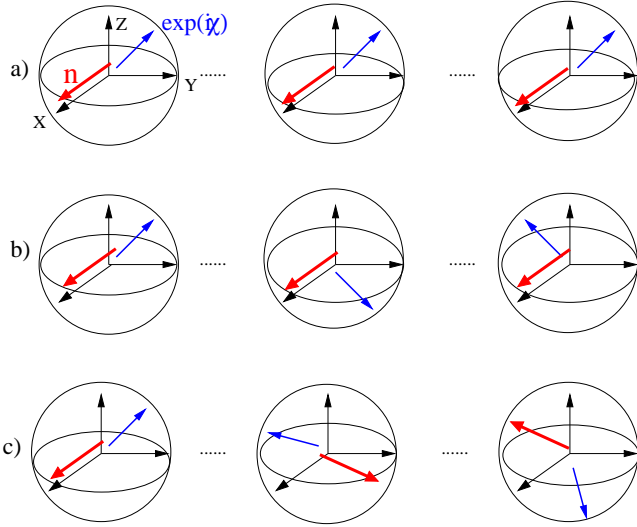


FIG. 1. Ordering of two order parameters, unit vectors \mathbf{n} (a light arrow defined on a two sphere S^2) and $\exp(i\chi)$ (a dark arrow defined on a unit circle S^1 , drawn in the YZ -plane of the two sphere) in different correlated states. a) pBEC, b) NMI and c) SSMI. Two spheres and unit circles (S^2 and S^1) for a few different lattice sites are shown here.

In terms of collective coordinates \mathbf{n}_k , the effective Hamiltonian for Mott insulating states can be expressed as

$$\mathcal{H}_{\text{MI}} = -J_{ex} \sum_{\langle kl \rangle} Q_{\alpha\beta}(\mathbf{n}_k) Q_{\alpha\beta}(\mathbf{n}_l) + E_s \sum_k \mathbf{S}_k^2; \quad (22)$$

$$Q_{\alpha\beta}(\mathbf{n}) = \mathbf{n}_\alpha \mathbf{n}_\beta - \frac{1}{3} \delta_{\alpha\beta}.$$

The exchange interaction J_{ex} is of the order of $t^2 E_c^{-1}$. The Hilbert space observes the following symmetry under a local inversion \hat{O}_k^n ,

$$\hat{O}_k^n \Psi_{N_0} = (-1)^{N_0} \Psi_{N_0}; \quad (23)$$

Finally, the Hamiltonian is invariant under the local inversion

$$(\hat{O}_k^n)^{-1} \mathcal{H}_{\text{MI}} \hat{O}_k^n = \mathcal{H}_{\text{MI}}. \quad (24)$$

In the limit of ii), one can identify the ground state as a nematic Mott insulator. In this intermediate regime, the director \mathbf{n} is localized on a two-sphere S^2 . The wavefunctions for an even (e) and odd (o) number of atoms per site are

$$\Psi_{\text{NMI}}^e(\{\mathbf{n}_k\}) \approx \prod_k \delta((\mathbf{n}_k \cdot \mathbf{n}_0)^2 - 1)$$

$$\Psi_{\text{NMI}}^o(\{\mathbf{n}_k\}) \approx \prod_k \delta((\mathbf{n}_k \cdot \mathbf{n}_0)^2 - 1)(\mathbf{n}_k \cdot \mathbf{n}_0). \quad (25)$$

One notices that

$$\hat{O}_k^n \Psi_{\text{NMI}}^e = \Psi_{\text{NMI}}^e, \quad \hat{O}_k^n \Psi_{\text{NMI}}^o = -\Psi_{\text{NMI}}^o \quad (26)$$

so that the constraint in Eq.23 is satisfied. Eq.25 indicates that at each site all localized atoms condense in an identical spin-one state characterized by $\psi_\alpha^\dagger \mathbf{n}_{0\alpha}$; microscopically (see Fig. 2a))

$$\Psi_{\text{NMI}}^{e,o} \approx \prod_k \frac{(\chi_{k\alpha}^\dagger \mathbf{n}_{0\alpha})^{N_0}}{\sqrt{N_0!}} |0\rangle \quad (27)$$

which corresponds to a maximally ordered state.

A direct calculation of order parameters defined in Eq.1 in section I yields

$$\text{pBEC} : \mathcal{O}_\alpha^1 = \sqrt{N_0} \mathbf{n}_\alpha \exp(i\chi_0);$$

$$\text{NMI} : \mathcal{O}_\alpha^1 = 0, \mathcal{O}_{\alpha\beta}^2 = N_0 (\mathbf{n}_\alpha \mathbf{n}_\beta - \frac{1}{3} \delta_{\alpha\beta}). \quad (28)$$

Nematic Mott insulating states can be observed at temperatures lower than the exchange energy J_{ex} .

Nematic states break the rotational symmetry. The internal space and its first homotopy group are

$$\mathcal{R} = \frac{S^2}{Z_2}, \pi_1(\mathcal{R}) = Z_2.$$

These states support interesting π -spin disclinations (some general discussions on the effects of Ising symmetry on atomic defects can be found in an early work [34]).

In the limit of iii), \mathbf{n} and χ are delocalized on the unit sphere S^2 and unit circle S^1 respectively; for an even number ($N_0 = 2n$) of particles per site, the wave function for a spin singlet Mott insulator (SSMI) can be written as

$$\Psi_{\text{SSMI}}^e(\{\mathbf{n}_k\}) \approx \prod_k Y_{0,0}(\mathbf{n}_k), \quad (29)$$

$Y_{0,0}$ is the zeroth spherical Harmonics. Ψ_{SSMI}^e is rotationally invariant unlike NMI or pBEC; the microscopic wave function which yields the desired collective behavior specified in this limit is (see Fig. 2b))

$$\Psi_{\text{SSMI}}^e \approx \prod_k \frac{(\chi_{k\alpha}^\dagger \chi_{k\alpha})^n}{\sqrt{(2n+1)!}} |0\rangle. \quad (30)$$

The situation for an odd number of atoms per site is more involved and will be discussed in the next section. As mentioned, more detailed discussions on quantum spin ordered or disordered phases can be found in two very recent works [14,15].

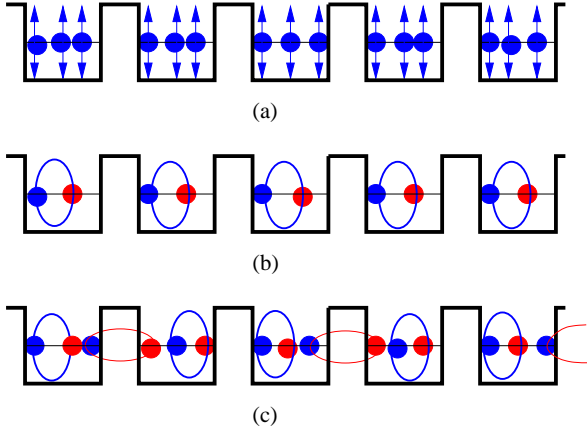


FIG. 2. Schematic of microscopic wave functions of an NMI (a), an SSMI for $N_0 = 2n$ (b) and a DVBC for $N_0 = 2n + 1$ (c). A dot carrying a double-headed director pointing in direction \mathbf{n} represents a spin-one boson in a state $\psi_{\alpha}^{\dagger} \mathbf{n}_{\alpha} |vac\rangle$; each pair of dark and light dots connected with a ring stands for a spin singlet pair of two spin-one atoms.

III. DVBCS IN ONE-DIMENSIONAL MOTT INSULATING STATES: SMALL HOPPING LIMIT

Consider one-dimensional Mott states when the hopping is much less than $E_{c,s}$. For an odd number ($N_0 = 2n + 1$) of atoms per site, each two unpaired atoms at two neighboring sites form a spin singlet and the ground state is a dimerized-valence-bond crystal state [19]. The previous results suggest the following wave functions (see Fig. 2c))

$$\Psi_{SSMI}^o \approx \prod_k' \frac{(\chi_{k\alpha}^{\dagger} \chi_{k\alpha}^{\dagger})^n (\chi_{(k+1)\alpha}^{\dagger} \chi_{(k+1)\alpha}^{\dagger})^n}{(2n+3)(2n+1)!} \chi_{k\beta}^{\dagger} \chi_{(k+1)\beta}^{\dagger} |0\rangle. \quad (31)$$

The product \prod_k' is carried over all odd sites ($k = 2m + 1$) or all even ones ($k = 2m$). Since the key idea of SSQCs is intimately connected with properties of DVBCs, in this section we will present evidence for DVBC states in one-dimensional lattices.

Though dimerization occurs in all one-dimensional Mott states for an odd number of particles per site, we start with a simple limit when

$$t \ll \sqrt{E_c E_s}, E_c; \quad (32)$$

we would like to demonstrate the origin of these dimerized states of spin-one atoms from the point of view of bilinear-biquadratic (BLBQ) spin models. Discussions on more general cases can be found in section VIII. The Hilbert space at each site is defined in Eqs.7-11. For odd numbers of bosons per site ($N_0 \gg 1$), the low energy Hilbert space for each isolated site is spanned by states of

total spin $S = 1, 3, 5, \dots$. Therefore, as E_s is much larger than t , one can further truncate the Hilbert space at each site into a space of a spin-one particle (see FIG.3).

The effective exchange interactions between two adjacent condensates can then be obtained by examining the excitation spectrum of two coupled sites. At $t = 0$, the ground state of two decoupled condensates has a nine-fold degeneracy. At any finite t much less than $E_{s,c}$, because of virtual hopping between two sites, the nine-fold degeneracy in the truncated space is lifted and the resultant spectrum is

$$E(S) = -\alpha_S J, S = 0, 1, 2; \quad (33)$$

α_S calculated for two coupled condensates are

$$\alpha_S = \frac{\gamma_1(S)}{1 - 4c_s} + \frac{\gamma_2(S)}{1 + 2c_s} + \frac{\gamma_3(S)}{1 + 8c_s}, \quad (34)$$

and

$$\begin{aligned} \gamma_1(0) &= \frac{1}{6}, \gamma_3(0) = \frac{2}{15}, \gamma_3(1) = \frac{1}{10}; \\ \gamma_2(2) &= \frac{2}{15}, \gamma_3(2) = \frac{7}{150}; \\ \gamma_2(0) &= \gamma_1(1) = \gamma_2(1) = \gamma_1(2) = 0. \end{aligned} \quad (35)$$

$c_s = E_s/E_c$; and α_0 is always larger than $\alpha_{1,2}$.

The truncation can be carried out in a similar way in a lattice. The following reduction in dimensions of the Hilbert spaces takes place when the hopping is weak

$$\mathcal{D}_0 = \left[\frac{(N_0 + 1)(N_0 + 2)}{2} \right]^{V_T} \rightarrow \mathcal{D}_T = 3^{V_T}. \quad (36)$$

Here V_T is again the number of sites in a lattice and the number of bosons at each side N_0 is much larger than one. In the truncated Hilbert space of dimension \mathcal{D}_T , Eq.33 suggests the following effective Hamiltonian

$$\mathcal{H}_{eff} = - \sum_{\langle kl \rangle} \sum_S J \alpha_S \mathcal{P}_S(\mathbf{S}_k, \mathbf{S}_l) \quad (37)$$

where $\mathcal{P}_S(\mathbf{S}_k, \mathbf{S}_l)$ is a projection operator for a total spin S state of two condensates at neighboring sites k and l ($\mathbf{S}_k^2 = \mathbf{S}_l^2 = 2$).

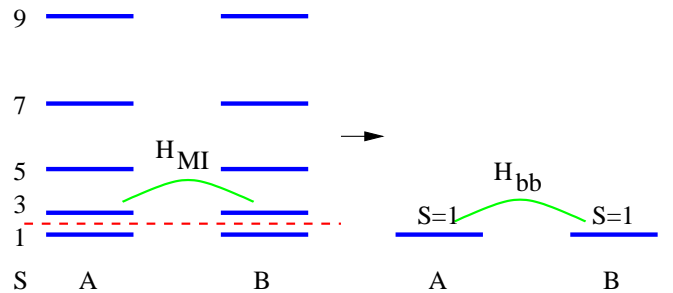


FIG. 3. The truncation of the Hilbert space of two condensates A and B ($N_0 = 2n + 1$) when t is much less than $E_{c,s}$. The effective Hamiltonian in the truncated space is $\mathcal{H}_{b.b.}$.

For one-particle per site ($N_0 = 1$) at small hopping limit, a straightforward calculation yields values of α_S , $S = 0, 1, 2$,

$$\alpha_1 = 0, \alpha_0 = \frac{4}{1 - 2c_s}, \alpha_2 = \frac{4}{1 + c_s}.$$

and again $\alpha_0 > \alpha_2 > \alpha_1$.

Now we can proceed to one-dimensional lattices where the situation is relatively well understood. For an odd number of bosons per site ($N_0 = 2k + 1$), the Mott insulating state should be a DVBC with a twofold degeneracy [19]. To obtain this result, we take into account the peculiar property of the truncated Hilbert space and energy spectrum. Following Eq.37, one shows that the problem of interacting spin-one bosons with an odd number of bosons per site can be mapped into the BLBQ spin-one spin chain model.

$$\frac{\mathcal{H}_{\text{b.b.}}}{J} = \cos \eta \sum_{\langle ij \rangle} \mathbf{S}_i \cdot \mathbf{S}_j + \sin \eta \sum_{\langle ij \rangle} (\mathbf{S}_i \cdot \mathbf{S}_j)^2, \quad (38)$$

if η satisfies $\tan \eta = (\alpha_1 - \frac{1}{3}\alpha_2 - \frac{2}{3}\alpha_0)(\alpha_1 - \alpha_2)^{-1}$ and the sign of $\sin \eta$ is chosen to be the same as $\alpha_1 - \frac{1}{3}\alpha_2 - \frac{2}{3}\alpha_0$. c_s varies from 0 to 1/4 when $N_0 = 2k + 1 \gg 1$, and from 0 to 1/2 when $N_0 = 1$; consequently, η varies as

$$-\frac{\pi}{2} > \eta > \eta_0. \quad (39)$$

The value of η_0 in general depends on models used in different limits; for the large- N_0 case ($N_0 = 2k + 1 \gg 1$), $\eta_0 = -\frac{\pi}{2} - \arctan \frac{1}{2}$ while for $N_0 = 1$, $\eta_0 = -3\pi/4$. For parameters given in Eq.39, following discussions in [40] we arrive at conclusions that the ground states should be dimerized valence bond crystals or DVBCs. The wave function of DVBCs for $N_0 = 2k + 1$ atoms per site is proposed at the beginning of this section. At $\eta = 0$, the model describes a Heisenburg antiferromagnet; solutions in this limit were also studied in [53].

Taking into account Eqs.8,31, one obtains spin-spin correlations in DVBC states. The DVBC state breaks the crystal translational symmetry and has a twofold degeneracy; one of degenerate states is characterized by the following correlation functions ($m \neq n$)

$$\begin{aligned} \langle \mathbf{S}_m \cdot \mathbf{S}_n \rangle &\propto -\frac{1}{8}(1 - (-1)^m)(1 + (-1)^n)\delta_{n,m+1}, \\ \langle \mathbf{S}_m \cdot \mathbf{S}_{m+1} \mathbf{S}_n \cdot \mathbf{S}_{n+1} \rangle &\propto \frac{1}{16}(1 - (-1)^m)(1 - (-1)^n). \end{aligned} \quad (40)$$

Because of the selection rule discussed in Eq.11 in section II, for even numbers of bosons per site, the Hilbert space is spanned by states with total spins of $S = 0, 2, 4, \dots, N_0$. The lowest energy space can be truncated into a spin singlet state. As the coupling t between sites is much smaller than E_s , the exchange interaction

is an irrelevant operator; the ground state remains to be a non-degenerate spin singlet Mott insulator as far as t is much smaller than E_s . In this limit, spin-spin correlations for $m \neq n$ are zero, i.e.

$$\langle \mathbf{S}_m \cdot \mathbf{S}_n \rangle \approx 0. \quad (41)$$

IV. EXCITATIONS IN SSMIS

In this section, we will demonstrate **charge-e** and **charge-2e** excitations. The existence of spinless but charge e ($S = 0, Q = 1$) excitations which do not carry full identities of spin one-bosons implies the fractionalization of spin-one atoms. These spinless objects also provide important hints on microscopic wave functions of SSQCs discussed in the next section.

A. Charge-e excitations in one-dimensional DVBCs

In terms of creation operators of a valence bond at link η which connects two neighboring sites i and j

$$\phi_\eta^\dagger = \frac{1}{\sqrt{3}}(\mathbf{h}_{i,1}^\dagger \mathbf{h}_{j,-1}^\dagger + \mathbf{h}_{i,-1}^\dagger \mathbf{h}_{j,1}^\dagger - \mathbf{h}_{i,0}^\dagger \mathbf{h}_{j,0}^\dagger), \quad (42)$$

the wave function of one-dimensional DVBC states can be written as

$$\Psi_{\text{DVBC}} = \prod' \phi_\eta^\dagger. \quad (43)$$

The product \prod' is carried over all even or odd links; $\mathbf{h}_{i,m}^\dagger$ is a creation operator of a condensate at site i with total spin $S = 1$, $S_z = m$.

A one-dimensional DVBC state supports two kinds of elementary excitations which are of topological nature [19]. A spinless but "charge-e" excitation ($Q = 1, S = 0$) represents a spin singlet state with an extra atom compared with the Mott ground state; a chargeless but spinful excitation ($Q = 0, S = 1$) on the other hand is a spin-one state but with the same number of atoms as the Mott state. Both excitations are kink-like and created only by nonlocal operators.

An $S = 1, S_z = m$ excitation can be created by the following product operator

$$\mathcal{C}_{\gamma,m}^\dagger = \mathcal{P}_{G.G.}^1 \mathbf{h}_{\gamma,m}^\dagger \prod_{\eta \in \mathcal{C}_\gamma} [\phi_\eta^\dagger + \phi_\eta]. \quad (44)$$

The product is carried over all links η along path \mathcal{C}_γ which starts at site γ and ends at infinity; furthermore, \mathcal{C}_γ is chosen such that the first link along the path is occupied by a valence bond. $\mathcal{P}_{G.G.}^n$ is a generalized Gutzwiller projection to project out states with n -particles per site. Therefore, Eq.44 indeed represents a spin-one domain

wall soliton ($m(S_z) = 0, \pm 1$) located at site γ in the DVBC state as shown in Fig.4a).

The hopping matrix of domain-wall along an one-dimensional lattice is

$$\mathcal{T}_{ij} = -\frac{1}{3}\alpha_0[\delta_{i,j-2} + \delta_{i,j+2}].$$

Taking it into account, we obtain the following band structure for spin-one excitations;

$$E(Q_x) = J\alpha_0\left(1 - \frac{2}{3}\cos 2Q_x\right) \quad (45)$$

with Q_x defined as a crystal momentum of excitations, $-\pi/2 < Q_x < \pi/2$. These excitations are purely magnetic and involve no extra bosons; therefore are "neutral" ($Q = 0$).

Besides spin-one "neutral" excitations, there are also "charged" spinless ($S = 0, Q = 1$) domain wall excitations. A "charged" excitation with a positive or negative charge ($Q = \pm 1$) is defined by a creation operator $B_{\gamma,\pm}^\dagger$ and

$$C_{\gamma,m}^\dagger = \psi_{\gamma,-m}B_{\gamma,+}^\dagger = \psi_{\gamma,m}^\dagger B_{\gamma,-}^\dagger, \quad (46)$$

$\psi_{i,m}^\dagger(\psi_{i,m})$ is a creation (annihilation) operator for a spin-one atom with $S_z = m$. The situation in one-dimensional optical lattices is therefore similar to conducting polymers [54].

The splitting of the low energy Hilbert space suggests the fractionalization of atoms. It also suggests a possible quantum condensate of fractionalized particles of charge-e. Following Eq.46, as it is added to an one-dimensional DVBC, a spin-one atom fractionalizes into a spin-zero domain wall (with an extra atom thus "charged") and a spin- one "neutral" domain wall because of the twofold degeneracy for $N_0 = 2n + 1$ atoms per site.

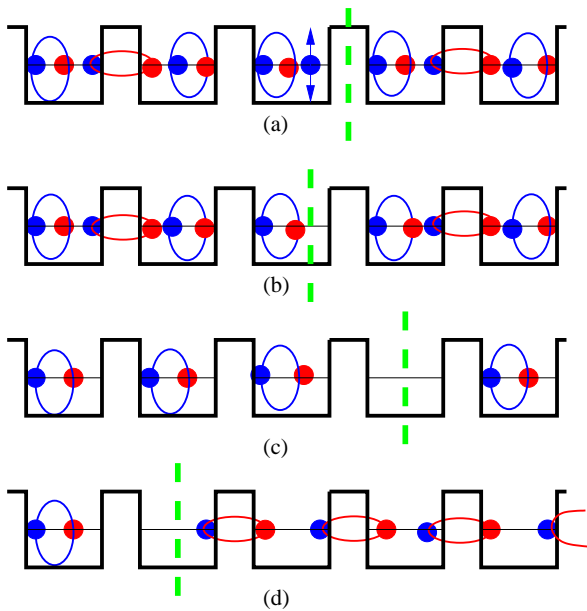


FIG. 4. Microscopic wave functions of excitations in one-dimensional optical lattices. a) A spin-one kink excitation ($S = 1, Q = 0$) in a DVBC; b) A charge-e excitation ($Q = 1, S = 0$) in a DVBC; c) A charge-2e excitation ($Q = 2, S = 0$) in an SSMI for an even number of atoms per site. In d), we also show an $S = 0, Q = 1$ state in an SSMI ($N_0 = 2n$); creation of this state results in a string of singlet bonds and is an energetic catastrophe. Locations of excitations are indicated by dashed lines.

B. Charge-2e excitations in one-dimensional SSMIs

The only spinless excitations in one-dimensional SSMIs for an even number of atoms per site are charge-2e ones. To demonstrate it microscopically, one considers a limit when E_s is infinity. All singlet pairs are bound and elementary charge excitations are charge-2e objects. At large but finite E_s , one finds at each site, the only spinless excitations are created by adding or removing singlet pairs with $Q = 2$ and $S = 0$. These again correspond to charge-2e excitations.

V. A PROJECTED SPIN SINGLET HILBERT SPACE BASED APPROACH

To apprehend the key physics in SSMIs and SSQCs, we first provide an intuitive approach to this problem. In a projected Hilbert space, we are going to demonstrate that the problem of spin-one bosons with antiferromagnetic interactions can be mapped into spinless bosons interacting with Ising gauge fields.

Let us consider a projected spin singlet Hilbert space which satisfies the following conditions:

- a) each atom has to form a spin singlet with another one either at the same site or a nearest neighboring site;
- b) each link has to be occupied by at most one spin singlet pair of atoms (a valence bond).

c) Following a), b), the parity of the number of valence bonds emitted from a lattice site is the same as that of the number of particles at that site. For instance, for a site with one particle, one of the links connected to that site has to be occupied by a valence-bond. For a site with two particles, either two or none of the links are occupied by valence-bonds.

In Fig.5, we show examples of states in this projected Hilbert space. We employ a valence bond counting operator

$$\hat{d}_{k,k+1} = \frac{1 - \sigma_{k,k+1}^x}{2} \quad (47)$$

at each link $\eta = (k, k + 1)$, the eigen values of which are $d_{k,k+1} = 0, 1$. So we define the projected spin spin singlet

Hilbert space as the one constructed out of eigenstates of $\{\hat{\rho}_k\}$ and $\{\hat{d}_{k,k+1}\}$

$$|\dots\rho_k, d_{k,k+1}, \rho_{k+1}\dots\rangle, \text{ if } (-1)^{\rho_k + \sum_{\eta} d_{\eta}} = 1. \quad (48)$$

Here ρ_k is the number of particles at site k , $d_{k,k+1}$ is the number of valence bonds at a link connecting site k and $k+1$. The local constraint in Eq.48 follows point c) discussed above; η represents a link connected to site k .

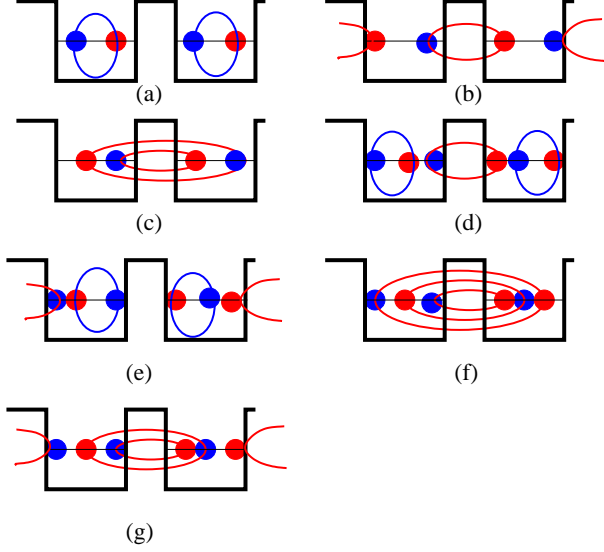


FIG. 5. Examples of states in a projected spin singlet Hilbert space. a), b) and d), e) are states in this space. States in c) or f) and g) can be "deformed", respectively, into states in a) or d) and e) by locally breaking valence bonds and constructing intra-site singlets without involving atoms at a third site. States in c), f) and g) have higher energies than their counterparts in a), d) and e) and do not belong to the projected Hilbert space. In a)-g) dots connected by rings are spin singlet pairs of spin-one bosons.

Consider hopping of an atom between two neighboring sites k, l (an even number of atoms per site in initial states, see Fig. 6a).

$$\begin{aligned} & \chi_{l\alpha}^\dagger \chi_{k\alpha} \frac{(\chi_{k\alpha_1}^\dagger \chi_{k\alpha_1}^\dagger)^n}{\sqrt{(2n+1)!}} \otimes \frac{(\chi_{l\alpha_2}^\dagger \chi_{l\alpha_2}^\dagger)^n}{\sqrt{(2n+1)!}} \\ & \rightarrow \chi_{k\alpha}^\dagger \frac{(\chi_{k\alpha_1}^\dagger \chi_{k\alpha_1}^\dagger)^{n-1}}{\sqrt{(2n-1)!}} \otimes \chi_{l\alpha}^\dagger \frac{(\chi_{l\alpha_2}^\dagger \chi_{l\alpha_2}^\dagger)^n}{\sqrt{(2n+1)!}}. \end{aligned} \quad (49)$$

In a projected Hilbert space, hopping of atoms simply leads to transitions between the following states $|\dots\rho_k, d_{k,k+1}, \rho_{k+1}\dots\rangle$

$$\begin{aligned} & |\dots\rho_k, d_{k,k+1}, \rho_{k+1}\dots\rangle \rightarrow \\ & |\dots\rho_k - 1, 1 \mp d_{k,k+1}, \rho_{k+1} + 1\dots\rangle \end{aligned} \quad (50)$$

for $d_{k,k+1} = 1$ or 0 in initial states. One obtains an effective description of hopping of spin-one atoms in the projected Hilbert space.

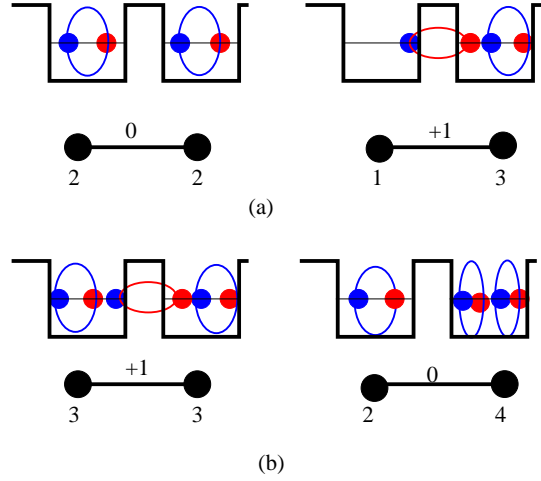


FIG. 6. Hopping of atoms in spin singlet Mott states and its effective description. For an even number of particles per site in a), hopping of an atom adds a singlet bond between two sites; in the lower part of a), this process is represented by changes in "charges", $b_k^\dagger b_k$ at each site (numbers below dots) and "countings" of valence bonds \hat{d}_η at each link (numbers above links). b) is for an odd number of particles per site. Notice that the parity of $\sum_{\eta} \hat{d}_\eta + b_k^\dagger b_k$ at each site is conserved when atoms hop around; η is a link connected with site k . The description in a) and b) leads to an effective theory on spin-one atoms in 1D lattices. In a) and b), we only keep states in the projected Hilbert space introduced in this subsection.

Moreover, at zero hopping, energies of states with different particles are given by "charging" energies in Eq.6. And to create valence bonds one needs to break intra site singlet pairs; and thus the energy cost of a valence bond is E_s if J_{ex} is much smaller than E_s . Therefore in the projected Hilbert space $|\dots\rho_k, d_{k,k+1}, \rho_{k+1}\dots\rangle$, we obtain the following mapping

$$\begin{aligned} & t\chi_{k\alpha}^\dagger \chi_{l\alpha} \rightarrow tb_k^\dagger b_l \sigma^z; \\ & \rho_k \rightarrow b_k^\dagger b_k, \frac{\rho_k^2}{2C} \rightarrow \frac{\rho_k^2}{2C}; \\ & \frac{S_k^2}{2I} \rightarrow 2\Gamma_b \hat{d}_\eta. \end{aligned} \quad (51)$$

(using σ^z as a linear combination of raising and lowering operators defined with respect to \hat{d}). The resultant Hamiltonian is the same one as in Eq.103, which will be derived in a more formal way. It is easy to confirm that $\Gamma_b \sim E_s$ when $E_s \gg J_{ex}$.

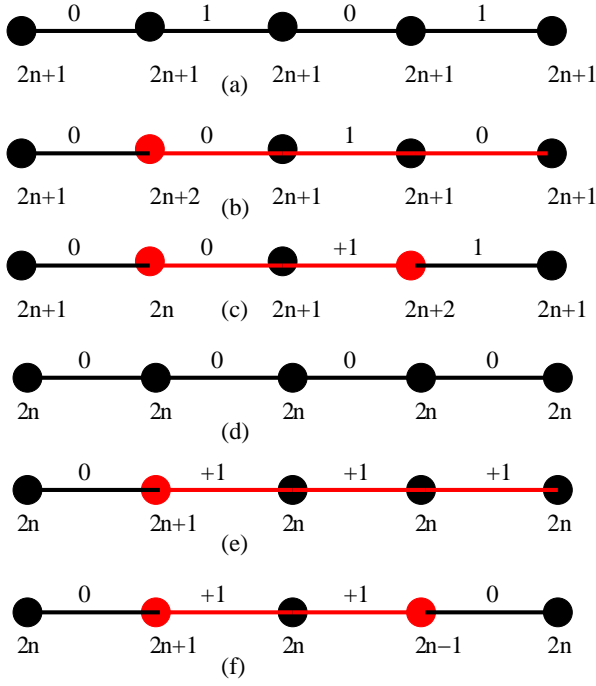


FIG. 7. Schematic of one dimensional SSIs and hopping of bosons in these states. a) a DVBC for an odd number of particles per site; b) an $S = 0$ and $Q = 1$ kink excitation in a DVBC; c) hopping of an atom results in a kink-anti kink pair; d) an SSMe for an even number of particles per site; e) an $S = 0$ and $Q = 1$ "excitation" in an SSI (for $N = 2n$) emitting a string of valence bonds; f) hopping of a boson is suppressed in an SSI (for $N = 2n$) because of a string of valence bonds between particle-hole excitations. Numbers appearing at each link are countings of \hat{d} and those below dots are numbers of particles at each site; light dots are "charged" and along light links valence bonds have been removed or added to ground states.

The effective Hamiltonian is convenient for the study of spin singlet states. Let us consider spin singlet Mott insulating states discussed in section II,III; In the projected space, when $E_s \gg J_{ex}$, ground states can be read out as

$$\begin{aligned} \rho_k &= 2n + 1, d_{k,k+1} = \frac{1}{2}(1 \pm (-1)^k), \text{ for } N_0 = 2n + 1; \\ \rho_k &= 2n, d_{k,k+1} = 0, \text{ for } N_0 = 2n \end{aligned} \quad (52)$$

as illustrated in Fig.7a) and 7d).

The effective Hamiltonian in the projected spin singlet Hilbert space is also particularly useful for the discussion of hopping of atoms across lattices. Following the constraint in Eq.47, the insertion of an atom to site k changes ρ_k by one unit and leads to an $S = 0, Q = 1$ kink-like excitation (see Fig.7b)); this reproduces an spin singlet charge-e excitation in Fig.4b). On the other hand, for an even number of particles per site, adding an atom to a site results in an $S = 0$ and $Q = 1$ string-like excitation (see Fig.7 e)), this was also discussed in Fig.4d).

This difference between lattices with even or odd numbers of particles per site mentioned above plays a remarkably important role when hopping is taken into account. In Fig.7, we illustrate hopping of atoms schematically from this point of view. Hopping of atoms in an "odd" lattice results in kink-anti kink pairs which are weakly interacting. *However, in an "even" lattice hopping is strongly suppressed because of strings of valence bonds created between particle and hole excitations as shown in Fig.7 f)*; it implies that only pairs of atoms or charge-2e objects propagate along the lattice in this case. In the following sections, we implement this idea more quantitatively using some properties of Ising gauge fields.

Similar analysis about one-particle hopping in spin singlet states can be easily carried out in high dimensional lattices. For even numbers of atoms per site, one arrives at the same conclusions as in one dimensional lattices. For odd numbers of atoms per site, using the mapping argued in this section, one can also investigate hopping in possible DVBC states in square lattices (see Appendix A).

VI. A FRACTIONALIZED REPRESENTATION

For a discussion on SSQCs or more general fractionalized quantum condensates (FQCs), we find that it is most convenient to introduce a representation involving "chargeless" ($Q = 0$) spin-one operators \mathbf{a}_α and "spinless" ($S = 0$) **charge-e**($Q = 1$) operators b ;

$$\mathbf{a}_{k\alpha}^\dagger = b_k \chi_{k\alpha}^\dagger. \quad (53)$$

\mathbf{a} , b , $\hat{\rho}$ and \mathbf{S} satisfy the following algebras

$$\begin{aligned} [\rho_k, b_l^\dagger] &= \delta_{kl} b_k^\dagger, [\hat{\rho}_k, \mathbf{a}_l^\dagger] = 0 \\ [\mathbf{S}_k^\alpha, \mathbf{a}_{l\beta}^\dagger] &= i\epsilon^{\alpha\beta\gamma} \delta_{kl} \mathbf{a}_{k\gamma}^\dagger, [\mathbf{S}_k^\alpha, b_l^\dagger] = 0. \end{aligned} \quad (54)$$

Eq.53 suggests that

$$\hat{\rho}_k = b_k^\dagger b_k, \mathbf{S}_{k\alpha} = -i\epsilon_{\alpha\beta\gamma} \mathbf{a}_{k\beta}^\dagger \mathbf{a}_{k\gamma};$$

the spin density is carried by \mathbf{a} -particles, or spin-one *spinons* and charge density is carried by b -particles, or *chargons*. It implies a possibility of spin-"charge" separation in cold atoms. General discussions on spin-charge separation in strongly correlated electrons can be found in [27,28,30–33,37–49].

Obviously, the enlarged Hilbert space spanned by $\{\mathbf{a}^\dagger\}$ and $\{b^\dagger\}$ includes unphysical states violating the symmetry of many-boson wave functions. Because of the symmetry constraint, all physical low energy states have to display a superselection rule discussed in details in section II. Namely, for an even number of atoms N_0 , the low energy Hilbert space is occupied by states with $S = 0, 2, 4, 6, \dots, N_0$ while for an odd N_0 , the Hilbert space is spanned by states with $S = 1, 3, 5, \dots, N_0$.

Following the identity in Eq.10, if one has an even number of \mathbf{a}^\dagger -particles, resultant total spins are $S = 0, 2, 4, \dots$ and for an odd number, spin states are those with $S = 1, 3, 5, \dots$. To produce desired symmetric states of spin-one atoms, one has to require at least that the total numbers of \mathbf{a} - and b - particles, or spinons and chargons, be even. If the average numbers of \mathbf{a} - and b - particles at each site are much larger than one, it is possible to generate correct low energy Hilbert spaces by imposing the following constraint so that for every state Ψ ,

$$\hat{C}_k \Psi = \Psi, \hat{C}_k = \exp(\pm i\pi[\mathbf{a}_k^\dagger \cdot \mathbf{a}_k + b_k^\dagger b_k]). \quad (55)$$

The constraint in Eq.55 is precisely to exclude the unphysical states in the enlarged space spanned by b^\dagger and $\mathbf{a}_\alpha^\dagger$ which violate the selection rule in Eq.11.

Considerations based on previous works on discrete gauge symmetries [34,11] indicate that the Hamiltonian in Eq.6 should be equivalent to the following one in this fractionalized representation,

$$\mathcal{H}_{FR} = \sum_k \frac{\mathbf{S}_k^2}{2I} + \frac{\hat{\rho}_k^2}{2C} - \hat{\rho}_k \mu - \tilde{t} \sum_{\langle kl \rangle} (\mathbf{a}_{k\alpha}^\dagger \mathbf{a}_{l\alpha} b_k^\dagger b_l + \text{h.c.}), \quad (56)$$

In appendix B, we provide further evidence for the equivalence between Eq.56 and Eq.6.

Let us emphasize that we are interested in the following limit where the equivalence has been established;

$$\langle \hat{\rho}_{kb} \rangle = N_0, \langle \hat{\rho}_{k\mathbf{a}} \rangle = N_{\mathbf{a}} \quad (57)$$

and both N_0 and $N_{\mathbf{a}} (\ll N_0)$ are much larger than unity.

$$\hat{\rho}_{kb} = b_k^\dagger b_k, \hat{\rho}_{k\mathbf{a}} = \mathbf{a}_{k\alpha}^\dagger \mathbf{a}_{k\alpha};$$

N_0 is the number of spin-one particles at each site determined by the chemical potential; the exact value of $N_{\mathbf{a}}$ depends on the truncation of the low energy Hilbert space and is not important for the rest of discussions.

The resultant Hamiltonian is invariant under a local gauge transformation

$$\hat{C}_k^{-1} \mathcal{H}_{FR} \hat{C}_k = \mathcal{H}_{FR}. \quad (58)$$

We should also emphasize here that only bilinear operators of $\mathbf{a}_k^\dagger, b^\dagger$ are invariant under the local gauge transformation defined in Eqs.55,58,

$$\begin{aligned} \hat{C}_k^{-1} \mathbf{a}_{k\alpha}^\dagger \mathbf{a}_{k\beta}^\dagger \hat{C}_k &= \mathbf{a}_{k\alpha}^\dagger \mathbf{a}_{k\beta}^\dagger, \\ \hat{C}_k^{-1} \mathbf{a}_{k\alpha}^\dagger b_k^\dagger \hat{C}_k &= \mathbf{a}_{k\alpha}^\dagger b_k^\dagger, \\ \hat{C}_k^{-1} b_k^\dagger b_k^\dagger \hat{C}_k &= b_k^\dagger b_k^\dagger. \end{aligned} \quad (59)$$

On the other hand, all linear operators transform non-trivially under this transformation;

$$\begin{aligned} \hat{C}_k^{-1} \mathbf{a}_{k\alpha}^\dagger \hat{C}_k &= -\mathbf{a}_{k\alpha}^\dagger, \\ \hat{C}_k^{-1} b_k^\dagger \hat{C}_k &= -b_k^\dagger. \end{aligned} \quad (60)$$

From a standard point of view, these linear operators carry charges defined with respect to the gauge transformation in Eq.55 while bilinear operators in Eq.58 are charge neutral.

This property of "fractionalized particles" is more explicit if we examine the corresponding action of the Hamiltonian derived in appendix B. Besides spinons and chargons, we also have introduced discrete gauge fields σ^x defined at links of the lattices [55–58]. The constraint discussed above results in Ising gauge fields $\sigma^x_{kl} = \pm 1$ in $D + 1$ Euclidean space. And

$$\begin{aligned} \sigma_{kl}^z &= \frac{1}{2i}(\sigma_{kl}^\dagger - \sigma_{kl}^-), \\ \frac{1}{2}[\sigma_{kl}^x, \sigma_{k'l'}^\pm] &= \pm \delta_{kl,k'l'} \sigma_{kl}^\pm. \end{aligned}$$

Following appendix B, an inversion of $\mathbf{n} \rightarrow -\mathbf{n}$, or $\exp(i\chi) \rightarrow -\exp(i\chi)$ corresponds to a discrete gauge transformation $\mathbf{a} \rightarrow -\mathbf{a}$, or $b \rightarrow -b$. The action is therefore manifestly invariant under the following local Ising gauge transformation

$$b_k^\dagger \rightarrow \Omega_k b_k^\dagger, \mathbf{a}_k^\dagger \rightarrow \Omega_k \mathbf{a}_k^\dagger, \sigma_{kl}^z \rightarrow \Omega_k \sigma_{kl}^z \quad (61)$$

with $\Omega_k = \pm 1$.

As indicated here, \mathbf{a}^\dagger and b^\dagger are indeed matter fields carrying charges of Ising gauge fields. Taking into account minimal coupling between gauge fields and matter fields, alternatively we construct a Hamiltonian which explicitly involves gauge fields σ_{kl}^z , spinon fields \mathbf{a}_k^\dagger and chargon fields b_k^\dagger .

$$\begin{aligned} \mathcal{H}_{MG} &= \sum_k \frac{\mathbf{S}_k^2}{2I} + \frac{\rho_k^2}{2C} - \rho_k \mu \\ &- \tilde{t} \sum_{\langle kl \rangle} \sigma_{kl}^z (\mathbf{a}_{k\alpha}^\dagger \mathbf{a}_{l\alpha} + b_k^\dagger b_l + \text{h.c.}), \end{aligned} \quad (62)$$

The Hilbert space of the Hamiltonian in Eq.62 is again subject to the constraint in Eq.55. The Hamiltonian is invariant only under the following generalized transformation

$$\begin{aligned} \hat{C}'_k &= \hat{C}_k \otimes \exp\left(\pm i\pi \sum_+ \frac{1 - \sigma_{kl}^x}{2}\right), \\ (\hat{C}'_k)^{-1} \mathcal{H}_{MG} \hat{C}'_k &= \mathcal{H}_{MG}. \end{aligned} \quad (63)$$

The sum over the cross (+) is carried over all links connected with site k . Calculations indeed suggest that the low energy physics of the new Hamiltonian be the same as the one in Eq.6 [59]. Both Eq.56 and Eq.62 will be employed for discussions on FQCs and specifically SSQCs.

VII. SPIN SINGLET STATES IN HIGH DIMENSIONAL LATTICES

To facilitate discussions on SSMIs and SSQCs or more general FQCs, we introduce the following correlation functions

$$\begin{aligned}\mathcal{G}_{\alpha\beta}^{\mathbf{a}}(k, l) &= \langle \mathbf{a}_{k\alpha}^\dagger \mathbf{a}_{l\beta} \rangle_m \\ \mathcal{G}^b(k, l) &= \langle b_k^\dagger b_l \rangle_m\end{aligned}\quad (64)$$

evaluated at a fixed gauge similar to a "minimal gauge" suggested in [57]. In this gauge, the number of links where $\sigma_{kl}^z = -1$ is minimal for a given distribution of gauge fields. The two-point correlation functions in Eq.64 are expected to diagnose possible condensation in the spin or charge sector of the Hilbert space. In addition, we introduce local pairing order parameters

$$\begin{aligned}\Delta_{\alpha\beta}^{\mathbf{a}}(k, k) &= \langle \mathbf{a}_{k\alpha}^\dagger \mathbf{a}_{k\beta}^\dagger \rangle \\ \Delta^b(k, k) &= \langle b_k^\dagger b_k \rangle\end{aligned}\quad (65)$$

which are manifestly gauge invariant under the local gauge transformation defined in Eq.58.

We further assume that the two parameters

$$G_s = \frac{t}{E_s}, G_c = \frac{t}{E_c}$$

can be varied independently. Two critical values G_{sc}, G_{cc} are introduced below to facilitate discussions on SSQCs and SSMIs. For the purpose of demonstration, in this section we limit ourselves to lattices with an even number of bosons per site ($N_0 = 2n$), though a generalization using the scheme developed in section V is possible.

Large Hopping limit: $G_s > G_{sc}, G_c > G_{cc}$ Under this condition, both spinons and chargons condense and the ground state represents a *polar condensate* or pBEC. The gauge fields are screened and $\prod_{\square} \sigma^z = 1$ at each plaquette; here \square represents an elementary plaquette. There are two branches massless spin wave excitations in this rotational- symmetry-breaking state and one branch massless density mode. The ac Josephson oscillation frequency is precisely the difference between the chemical potentials of two condensates.

Intermediate Hopping limit I: $G_s > G_{sc}, G_c < G_{cc}$ When E_s is much less than E_c , this corresponds to a limit where $E_c G_{cc} > t > E_s G_{sc}$. Following the Hamiltonian, chargons are completely depleted from the condensate. We are particularly interested in a self-consistent solution where spin-one spinons "condense" one way or the other. States in this limits are incompressible and therefore naturally correspond to Mott insulating states; condensation of spinons leads to nematic long range order. Nematic Mott states were studied briefly in section II; in appendix C, we provide an alternative description on NMIs using this fractionalized representation.

Intermediate Hopping limit II: $G_s < G_{sc}, G_c > G_{cc}$ This limit can be relevant to atomic gases in high dimensional optical lattices, especially when E_s is not too small compared with E_c . We are going to present results in this case, for the completeness of analyses on SSQCs and more important to facilitate discussions on low dimensional optical lattices in the next section. This case represents a situation where $E_s G_{sc} > t > E_c G_{cc}$.

Discussions in this case can be carried out parallel to the previous case analyzed in appendix C. All spinful excitations are fully gapped; after integrating out these excitations, we obtain an effective Hamiltonian in terms of chargons

$$\begin{aligned}\mathcal{H}_{f_{qcb}} &= \sum_k \frac{\hat{\rho}_k^2}{2C} - \mu \hat{\rho}_k - \tilde{t} \sum_{\langle kl \rangle} (b_k^\dagger b_l \sigma_{kl}^z + h.c.) \\ &+ \Gamma_b \sum_{\langle kl \rangle} \sigma_{kl}^x - K_{sb} \sum_{\square} \prod_{\square} \sigma_{kl}^z.\end{aligned}\quad (66)$$

Γ_b, K_{sb} are again functions of t, E_s . K_{sb} is much less than Γ_b when G_s is small,

$$\frac{K_{sb}}{\Gamma_b} \ll 1 (\Gamma_b \sim 6E_s); \quad (67)$$

and expected to be divergent close to G_{sc} . The induced constraint on the Hilbert space is

$$\hat{C}_k^{fb} \Psi = \Psi, \hat{C}_k^{fb} = \exp \left(i\pi [b_k^\dagger b_k + \sum_+ \frac{1 - \sigma_{kl}^x}{2}] \right). \quad (68)$$

And the Hamiltonian is also locally invariant under the action of \hat{C}_k^{fb} ,

$$(\hat{C}_k^{fb})^{-1} \mathcal{H}_{f_{qcb}} \hat{C}_k^{fb} = \mathcal{H}_{f_{qcb}}. \quad (69)$$

If Γ_b is much less than K_{sb} , chargons condense and the phase coherence is maintained,

$$\mathcal{G}^b(k, k + \infty) \neq 0, \mathcal{G}_{\alpha\beta}^{\mathbf{a}}(k, k + \infty) = 0 \quad (70)$$

and the rotational symmetry is unbroken. This state is compressible but should have zero spin susceptibility at a low temperature limit. We define this state as a charge-e SSQC.

One can also carry out discussions on a limit when t is much less E_s , or

$$\frac{\Gamma_b}{K_{sb}} \gg 1. \quad (71)$$

And gauge fields σ^x are expected to be unity at each link over the whole lattice; under the constraint in Eq.55, the reduced Hilbert space is subject to a constraint

$$\hat{C}_k^b \Psi = \Psi, \hat{C}_k^b = \exp(i\pi b_k^\dagger b_k). \quad (72)$$

Thus, the low energy physics is determined by the pair hopping of chargons;

$$\mathcal{H}_{pb} = \sum_k \frac{\rho_k^2}{2C} - \mu \rho_k - \tilde{t}_2 \sum_{kl} (b_k^\dagger b_k^\dagger b_l b_l + h.c.),$$

$$(\hat{C}_k^b)^{-1} \mathcal{H}_{pb} \hat{C}_k^b = \mathcal{H}_{pb}. \quad (73)$$

and

$$\tilde{t}_2 \approx \frac{t^2}{\Gamma_b} (\Gamma_b \sim 6E_s). \quad (74)$$

When $t_2 = N_0^2 \tilde{t}_2 \gg E_c$, the ground state is a condensate of paired chargons; in terms of chargon-operator b^\dagger ,

$$|g_2\rangle = \prod_k \mathcal{P}_{N_0 \times V_T} \exp(\Phi_b^\dagger(0)) |0\rangle,$$

$$\Phi_b^\dagger(Q_0) = \Delta_0 \sum_q b_{Q_0+q}^\dagger b_{-q}^\dagger. \quad (75)$$

The projection operator $\mathcal{P}_{N_0 \times V_T}$ acting on a generalized BCS pairing wave function is to project out $N_0 V_T$ -particle states; N_0 and N_a are even numbers. Again, $\mathcal{G}_{\alpha\beta}^a(k, l)$ and $\mathcal{G}^b(k, l)$ vanish as $k - l$ approaches infinity but Eq.75 indicates

$$\Delta^b(k, k) = \frac{\Delta_0}{1 - \Delta_0^2} \quad (76)$$

in the ground state. Finally, we should emphasize that this charge-2e SSQC could be alternatively considered as condensation of "charged" soliton-anti soliton pairs from a point of view of section IV.

Small hopping limit: $G_s < G_{sc}$, $G_c < G_{cc}$

We are going to revisit the strong-coupling limit of spin-one atoms in Mott insulating states; we will employ the fractionalized representation to express the wave functions of SSMI. Discussions are limited to even numbers of bosons per site.

In a strong-coupling limit $G_s, G_c \ll 1$ and $t_1 \ll E_s$, $t_2 \ll E_c$, gauge fields of σ^x "condense". The Hilbert space of spinons and chargons explicitly satisfies a constraint $\hat{C}_k^a \hat{C}_k^b \Psi = \Psi$. (\hat{C}_k^a is defined in Appendix C.)

As t is much smaller than the interaction energies, the Hamiltonian commutes with local spin and number operators in the leading order of $E_{c,s}$;

$$[\mathcal{H}, \mathbf{S}_k^2] = [\mathcal{H}, \rho_k^2] \approx 0. \quad (77)$$

Therefore, the ground state should be an eigenstate of these two *local* operators and the wave function can be expressed as a projected BCS state of chargons

$$|g_3\rangle = \mathcal{P}_{G.G.}^{2n} |g_2\rangle \quad (78)$$

where $\mathcal{P}_{G.G.}^{2n}$ is a generalized Gutzwiller projection for $2n$ -chargons per site. One can show that $S_k^2 = 0$ for any k and Eq.78 represents a spin singlet Mott insulator (SSMI) studied in section II.

Before turning to SSQCs in one-dimensional lattices, we first revisit SSIMs in one-dimensional lattices to further understand the even-odd effect discussed in section

III. We are going to generalize previous results on one-dimensional SSIMs using mappings to an instanton gas model of Ising gauge fields and quantum dimer models.

VIII. SSIMS IN LOW DIMENSIONAL LATTICES: A GENERAL APPROACH

A. Instantons in Ising gauge fields

From the point of view of Ising gauge fields introduced in the previous section, distinct properties of Mott states for odd and even numbers of bosons per site discussed in section III can also be attributed to a topological term in the effective actions for even and odd numbers of bosons per site. In this section, we are going to revisit SSIMs in low dimensional lattices employing the effective descriptions introduced in section VI. We will reproduce results in section II and III; furthermore, in one-dimensional lattices we are going to generalize the previous results on DVBC states in the limit $t \ll \sqrt{E_s E_c}$ (see section III) to the entire Mott phase.

The quantum problem of the Hamiltonian \mathcal{H}_{FR} , or equivalently the Hamiltonian of constrained quantum rotor model \mathcal{H}_{CQR} defined in d dimensions can be mapped into the following model in $(d+1)$ dimensions (appendix B),

$$\mathcal{H}_{FR} \longleftrightarrow \mathcal{H}_{CQR} \rightarrow O(2) \otimes O(3) \otimes Z_2. \quad (79)$$

The $O(2) \otimes O(3)$ non-linear sigma model characterizes the dynamics of two variables $\mathbf{n}, \exp(i\chi)$ introduced in section II, or spinons \mathbf{a}^+ and chargons b^+ in discussed in section VI.

In high dimensional lattices when t is much less than E_s and E_c , spinons don't condense and chargons are localized because of repulsive interactions; and the director \mathbf{n} becomes disordered as suggested by a renormalization group equation analysis on the $O(3)$ nonlinear sigma model. For an even number of atoms per site, this strong coupling fixed point can be confirmed by directly solving the Hamiltonian \mathcal{H}_{MI} in the same limit in all dimensions. In one-dimensional lattices, spin-one spinons again do not condense and the director \mathbf{n} is quantum disordered at any finite E_s because of long range fluctuations.

For an odd number of atoms per site in the absence of hopping, the low energy space is highly degenerate (see section III) and the situation is more delicate. On the other hand, from the point of view of effective actions, the difference in numbers of atoms per site is only reflected in a Berry's phase term (see Appendix B). As far as low dimensional lattices are concerned, we speculate that this topological term doesn't alter the renormalization group flow of the $O(3)$ -model and arrive at the conclusion that for an odd number of atoms per site, spinons also do

not condense and the director \mathbf{n} is also disordered as the strong-coupling limit is approached [60]. This observation at least can be justified in one-dimensional lattices by comparing the results obtained below and the ones presented in section III.

In this paper, we would like to assume a quantum disordered phase in square lattices for odd numbers of atoms per site because of certain frustration. For discussions on square lattices with odd numbers of atoms per site, we will take this as a starting point and analyze disordered phases in section VIII B3.

In the strong coupling limit where the hopping integral is much less than $E_{s,c}$, after integrating over $O(2)$ and $O(3)$ degrees of freedom, or chargons and spinons, one obtains an effective low energy theory,

$$\mathcal{S} = -k_\tau \sum_{\square} \prod_{\square} \sigma_{kl}^z - k_s \sum_{\square} \prod_{\square} \sigma_{kl}^z + iN_0 \frac{\pi}{2} \sum_r (1 - \sigma_{rk+\epsilon}^z). \quad (80)$$

σ_{kl}^z is an Ising field defined at each link kl ; \square is an elementary plaquette in a $(1+d)$ D Euclidean space. \sum^s and \sum^τ are carried over spatial plaquettes and plaquettes involving temporal links respectively. $k_{s,\tau}$ can be estimated using a high temperature expansion

$$k_s \sim (\epsilon t)^4, k_\tau \sim \max\left(\frac{t^2}{E_c^2}, \frac{t^2}{E_s^2}\right). \quad (81)$$

ϵ^{-1} is a high energy cut-off in our problem.

In one-dimensional lattices, the term proportional to k_s is absent; furthermore, the result in Eq.80 is valid as far as

$$t < G_{cc} E_c.$$

And therefore conclusions on one-dimensional lattices arrived in this section are expected to be valid for all one-dimensional Mott states disregarding the ratio between t and E_s .

It is worth emphasising that only the topological term explicitly depends on numbers of particles at each site. General effects of Berry's phases on spin liquids have been studied in various papers on strongly correlated electrons [53,26–30,33]. The topological term in Eq.80 indeed has rather surprising consequences on many-body ground state degeneracies and quantum numbers of excitations. In fact, this term determines the confining-deconfining property of effective Ising gauge fields in one-dimensional lattices. It can be easily appreciated in terms of suppression of instantons.

Consider a Z_2 -instanton in $(1+1)d$ Euclidean space which emits a string of negative bonds pierced by the x -axis so that the boundary condition along the temporal direction is periodic; only at the X_{th} plaquette shown in Fig.8,

$$\prod_{\square} \sigma_{ij}^z = -1; \quad (82)$$

otherwise the plaquette integral over an elementary square is one.

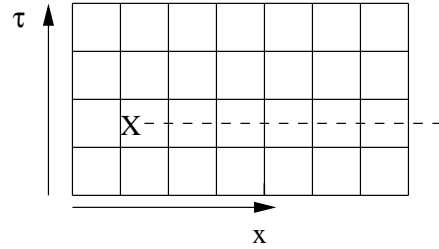


FIG. 8. A Z_2 -instanton located at X_{th} plaquette in $(1+1)$ D. At links pierced by the dashed line, $\sigma_{ij}^z = -1$.

Following the action in Eq.80, an instanton located at X th plaquette along the x -axis has a finite action and carries a phase

$$\Gamma_B = X\pi N_0. \quad (83)$$

In a dilute instanton gas limit ($o(e^{-k_\tau})$), the partition function of instantons is

$$\mathcal{Z}_{DIG} = \sum_n \frac{\beta^n}{n!} \sum_{\{X_1\}} \dots \sum_{\{X_n\}} \exp[-nk_\tau + i\pi \sum_{m=1}^n X_m N_0] \quad (84)$$

where the subscript m labels instantons. For $N_0 = 2n+1$, the sign of the amplitude of an instanton therefore alternates between positive and negative ones as the location of the instanton is shifted by one lattice constant a along the x -axis. A direct evaluation shows that in this case in the leading order of $o(e^{-k_\tau})$,

$$\frac{\ln \mathcal{Z}_{DIG}}{\beta L_x} \rightarrow 0 \quad (85)$$

as the perimeters along x and τ direction in the Euclidean space go to infinity. It suggests that instantons of Z_2 type should be absent in $(1+1)$ D because of destructive interferences [61].

The alternating sign of amplitude also implies that the ground state should break the crystal translational symmetry. Furthermore, the amplitude is periodical as a function of centers of instantons with a period of $2a$. So the ground state should develop a spin-Peirls structure with a period doubling that of underlying lattices. The suppression of instantons therefore appears to lead to unusual deconfining Ising gauge fields in $(1+1)$ D and a twofold degenerate spin-Peirls state, to which DVBCs

belong. For an even number N_0 , obviously instantons proliferate in the system and the ground state is non-degenerate and translationally invariant.

The instantons' behavior in this limit also determines quantum numbers of low lying *elementary* excitations, especially "topological" ones. For an odd number of bosons per site, a kink shown in Fig.4 should be an elementary spin-one excitation in the spectrum; this is indicated by the deconfining property of (frustrated) Ising gauge fields in (1+1)D. Thus, for an odd number of atoms per site, spin-charge separation takes place in any one-dimensional Mott state. On the other hand, for even numbers of atoms per site, gauge fields are confining. Lowest lying elementary excitations carry $S = 1$, $Q = 1$, or $Q = 0$, $S = 2$ or $S = 0$, $Q = 2$. The first one represents adding one atom to the system; the second type of excitations is to flip one spin singlet into $S = 2$ state and the last one is to add (or remove) a singlet pair of two spin one bosons (Fig.4c).

Generally, topological terms are known to play very important roles in quantum disordered states. In one-dimensional Heisenberg antiferromagnetic spin chains, topological terms lead to gapless spin liquids in half-integer spin chains, differing from an integer spin chain [53]. In 2D, topological terms can result in spin-Peirls states with different periodicity for half integer, odd and even integer Heisenberg antiferromagnets (disordered states) [26,27]. In the current situation the topological terms determine distinct quantum numbers of excitations for even or odd numbers of atoms per site.

B. Quantum dimer models

The Ising gauge fields describe the dynamics of low lying collective spin states of condensates at each site. Let us consider

$$\begin{aligned}\Sigma_{ij}^x &= \phi_{ij}^\dagger \phi_{ij} - \frac{1}{2}, \\ \Sigma_{ij}^y &= \frac{1}{2}(\phi_{ij}^\dagger + \phi_{ij}), \\ \Sigma_{ij}^z &= \frac{1}{2i}(\phi_{ij}^\dagger - \phi_{ij}), \\ \phi_{ij}^\dagger &= \frac{1}{\sqrt{3}}(\mathbf{h}_{i,-1}^\dagger \mathbf{h}_{j,1}^\dagger + \mathbf{h}_{i,1}^\dagger \mathbf{h}_{j,-1}^\dagger - \mathbf{h}_{i,0}^\dagger \mathbf{h}_{j,0}^\dagger)\end{aligned}\quad (86)$$

where ϕ_{ij}^\dagger is the creation operator of a singlet state of two adjacent condensates, or a valence bond; $\mathbf{h}_{m_F}^\dagger$ is a creation operator of a condensate with total spin one.

In a projected space of valence bond configurations where each link is occupied by at most one valence bond defined by ϕ_{ij}^\dagger , the Hilbert space at each link is an Ising doublet as pointed out in section V. One can easily confirm that Σ_{ij}^α , $\alpha = x, y, z$ satisfy the algebra of σ_{ij}^α and can be identified as σ_{ij}^α . So one interprets the effective action in terms of dynamics of valence bonds.

An interesting alternative but closely related point of view is the quantum dimer model [32]. The effective Hamiltonian of the Ising gauge fields in Eq.80 can be written as

$$\mathcal{H}_{IG} = -\Gamma \sum_{\langle kl \rangle} \sigma_{kl}^x - K_s \sum_{\square} \prod_{\square} \sigma^z \quad (87)$$

where the first sum is over all links and the second sum is over spatial plaquettes; and in one-dimensional lattices, the second term is absent. One can verify that the action of \mathcal{H}_{IG} is precisely that of the Ising gauge fields in Eq.80 [58]; indeed,

$$k_s = \epsilon K_s, k_\tau = -\frac{1}{2} \ln \tanh(\epsilon \Gamma). \quad (88)$$

When Γ is much smaller than K_s , k_τ becomes much larger than unity. On the other hand, k_τ is much less than the unity as Γ becomes much larger than K_s .

To generate desired topological terms in the action, we require that the Hilbert space satisfy the following local invariance at each site

$$\hat{g}_k \Psi = \Psi, \hat{g}_k = \exp[i\pi(\sum_{+} \frac{1 - \sigma_{kl}^x}{2} + N_0)], \quad (89)$$

for an even ($N_0 = 2n$) or odd number ($N_0 = 2n + 1$) of atoms each site. This constraint is identical to the constraint in Eq.48 which was derived from a very different consideration. The sum $+$ is carried over all links connected with site k . One can easily show that again for each site k

$$\hat{g}_k^{-1} \mathcal{H}_{IG} \hat{g}_k = \mathcal{H}_{IG}. \quad (90)$$

or \mathcal{H}_{IG} is locally invariant under the action of \hat{g}_k . The parity of the number of bosons enters the theory only in the definition of the Hilbert space.

At each link lives a two-dimensional Hilbert space $\sigma^x = \pm 1$. By assuming each link either occupied by a dimer ($\sigma^x = -1$) or empty ($\sigma^x = 1$), one introduces

$$\hat{d} = \frac{1 - \sigma^x}{2} \quad (91)$$

as a dimer counting operator (see also section V). The first term in \mathcal{H}_{IG} can be interpreted as the chemical potential of dimers. As σ^z is a linear combination of creation and annihilation operators of dimers, in square lattices the last term is the "kinetic" energy of dimers, which conserves the parity of numbers of dimers emitted from each site but does not conserve numbers of dimers. The connection between Ising gauge fields and quantum dimer model was recently illustrated in an interesting work [33].

The Hilbert space has four distinct sectors if periodical boundaries are imposed along both x and y -directions.

This aspect of the generalized model can be demonstrated explicitly in a torus or ring geometry. Let us introduce winding number operators

$$\hat{T}_{x,y} = \prod_{\mathcal{C}_{\infty}^{x,y}} (\sigma^x), \hat{T}_{x,y}^2 = 1. \quad (92)$$

Here $\mathcal{C}_{\infty}^{x(y)}$ is a path extending from $-\infty$ to $+\infty$ along the $x(y)$ -direction; the product is carried over all vertical links (y -direction) or horizontal links (x -direction) pierced by the path. Similar global operators were previously introduced for the study of correlated states [31,33].

It is easy to verify that for $i = x, y$,

$$[\hat{T}_i, \hat{T}_j] = 0, [\hat{T}_i, \mathcal{H}_{IG}] = 0. \quad (93)$$

$\hat{T}_i = \pm 1$ are good quantum numbers and the Hilbert space therefore has four sectors with different parities defined by $\hat{T}_{x,y}$. For a cylinder or a ring, one can only define \hat{T}_y if x is the direction of circumference. In this case, there are two sectors in the Hilbert space.

1. Even numbers of atoms per site in all bipartite lattices

Let us now turn to the ground states of the Hamiltonian in Eq.87. Solutions depend on the parity of numbers of bosons per site and we start with an even number of bosons per site. Following Eq.81, as t goes to zero, $k_{s,\tau}$ approach zero; therefore in this limit,

$$\frac{\Gamma}{K_s} \gg 1. \quad (94)$$

The relevant Hamiltonian is

$$\mathcal{H}_{qdm}^e = 2\Gamma \sum_{\eta} \hat{d}_{\eta} \quad (95)$$

which commutes with the dimer counting operator \hat{d}_{η} defined at each link η . The Hamiltonian is positive defined and the energy has a lower bound of zero. The ground state $|G^e\rangle$ obviously is a vacuum of dimers with $\hat{d} = 0$ at each link and is nondegenerate. In one-dimensional lattices, the ground state is

$$\hat{d}_{\eta}|G^e\rangle = 0, \hat{T}_y|G^e\rangle = |G^e\rangle. \quad (96)$$

where η is an arbitrary link.

In a torus, it has an even parity of $\hat{T}_{x,y}$; that is

$$\hat{d}_{\eta}|G^e\rangle = 0, \hat{T}_{x,y}|G^e\rangle = |G^e\rangle. \quad (97)$$

We identify this state as an SSMI state obtained in section II. The lowest excitations in this sector have energies 4Γ higher than the ground state. One can also show that the lowest energy states in $\hat{T}_x = -1$ or $\hat{T}_y = -1$ sector have energies proportional to the system size; they are not degenerate with the global ground state.

2. Odd numbers of atoms per site in 1D lattices

When t is much less than $E_{s,c}$ for an odd number N_0 , the low energy Hilbert space becomes spanned by configurations where only one of all links connected with each site is occupied by a dimer. In 1D, the second kinetic term in Eq.87 is absent and the constraint leads to a dimer crystal ground state with a twofold degeneracy. Particularly, two ground states $|G_{1,2}^o\rangle$ have different \hat{T}_y -parities

$$\hat{d}_{\eta}|G_{1,2}^o\rangle = \frac{1 \pm (-1)^{m_{\eta}}}{2}|G_{1,2}^o\rangle, \hat{T}_y|G_{1,2}^o\rangle = \pm|G_{1,2}^o\rangle. \quad (98)$$

Here m_{η} numerates link η in one-dimensional lattices. Interpreting each dimer as a valence bond, this point of view precisely leads to a dimerized-valence-bond crystal state.

3. Odd numbers of atoms per site in square lattices

For quantum spin disordered states in square lattices, one arrives at the following conclusions. For an odd number of atoms, the number of dimers from each site should be 1, 3, 5... etc; however, as Γ goes to infinity, the low energy Hilbert space is spanned by configurations with one dimer emitted from each site. Consequently, the constraint in this limit conserves the number of dimers emitted from each site and results in the following identity for any $U(1)$ gauge choice ϕ ,

$$\hat{h}_k = \exp[i\phi(\sum_{+} \hat{d}_{\eta} - 1)], \hat{h}_k \Psi = \Psi. \quad (99)$$

The mapping between a number conserved dimer model and a compact $U(1)$ theory was obtained in [45].

In square lattices, the constraint for $N_0 = 2n+1$ atoms per site therefore still leaves an exponentially large degeneracy in the low energy manifold; correspondingly, the kinetic energy in the Hamiltonian becomes

$$\mathcal{H}_{qdm}^o = -K_s \sum_{\square} \sigma^{\dagger} \sigma^{-} \sigma^{\dagger} \sigma^{-} + h.c. \quad (100)$$

in the reduced Hilbert space. This term lifts the residual degeneracy in the low energy manifold (σ^{\pm} are the raising and lowering operators defined in σ^x basis.); on the other hand, it preserves the reduced Hilbert space

$$\hat{h}_k^{-1} \mathcal{H}_{qdm}^o \hat{h}_k = \mathcal{H}_{qdm}^o. \quad (101)$$

Terms such as $\sigma^{\dagger} \sigma^{\dagger} \sigma^{\dagger} \sigma^{-}$, or $\sigma^{-} \sigma^{-} \sigma^{-} \sigma^{\dagger}$ are not invariant under the local $U(1)$ gauge transformation and have zero matrix elements in the space defined in Eq. 99.

It can be shown that the Hamiltonian acting on a reduced Hilbert space defined in Eq.99 is equivalent to the Rokhsar-Kivelson's quantum dimer model with $V = 0$ [33,32]. The ground states in a square lattice at $V = 0$ are column states with a fourfold degeneracy; furthermore, they break the crystal translational symmetry. This implies that a quantum disordered state in a square lattice should be a dimerized valence bond crystal state. For discussions on excitations, see appendix A.

To summarize, two main approaches have been employed to study spin correlated Mott insulating physics. The first one is using the effective Hamiltonian in reduced Hilbert spaces. The problem of interacting spin-one bosons is first mapped into a constrained quantum rotor model; spin correlations in Mott states then are studied using the Hamiltonian \mathcal{H}_{MI} introduced in section II. In the strong coupling limit when J_{ex} is much less than E_s , for an odd number of atoms per site, the Hamiltonian is further equivalent to the bilinear-biquadratic Hamiltonian $\mathcal{H}_{b.b.}$.

The second approach is to map the quantum problem into a classical one; the CQR problem can be mapped into a classical $O(2) \otimes O(3) \otimes Z_2$ model. In Mott states, the corresponding classical model is an $O(3) \otimes Z_2$ one, with a topological term. At the strong coupling limit, the model is also equivalent to constrained quantum dimer models. This mapping is employed to investigate disordered states in both one-dimensional and square lattices. For an odd number of particles per site, the later approach is used to generalize the results derived in the first approach to an intermediate hopping limit where the first approach is invalid.

At last, in square lattices, the effect of topological terms when N_0 is odd can be conveniently studied by a duality transformation from a constrained Ising gauge model to a fully frustrated Ising model in a transverse field [29,30,33,49]. The duality transformation indicates the ground state at infinit Γ limit should break the crystal translational symmetry. This again is consistent with the point of view of quantum dimer models.

IX. EVIDENCE FOR SSQCS IN ONE-DIMENSIONAL OPTICAL LATTICES

Following the analyses in section VI, it is clear that to have SSQCs in high dimensional lattices for integer numbers of particles per site, E_s has to be at least comparable to E_c . On the other hand, following analyses in [34], because of long wave length fluctuations, in one-dimensional lattices spin correlations are always short ranged; the rotational symmetry is unbroken (see Fig.9). Spin excitations are fully gapped for any finite value of E_s . For these reasons,

$$G_{sc} = +\infty. \quad (102)$$

For any hopping t and any E_s , G_s is always less than G_{sc} . Following discussions of **Intermediate Hopping limit II** in section VII, we therefore expect that when $G_c > G_{cc}$ or $t > E_c G_{cc}$, ground states must be condensates of fractionalized chargons, either charge-e SSQC or charge-2e SSQC. These condensates are spin singlets, differing from conventional pBECs discussed in high dimensional lattices (See Fig.9 and Fig.10).

The effective Hamiltonian for one-dimensional lattices can be written as

$$\begin{aligned} \mathcal{H}_{f_{qcb}}^{1d} = & -\tilde{t} \sum_{\langle kl \rangle} (b_k^\dagger b_l \sigma_{kl}^z + h.c.) \\ & + \sum_k \frac{\rho_k^2}{2C} - \mu \rho_k + \Gamma_b \sum_{\langle kl \rangle} \sigma_{kl}^x \end{aligned} \quad (103)$$

which differs from $\mathcal{H}_{f_{qcb}}$ in Eq.66 by a term involving spatial plaquettes. The Hilbert space of this Hamiltonian is subject to the same constraint as Eq.68

$$\hat{C}_k^{fb} \Psi = \Psi, \hat{C}_k^{fb} = \exp \left(i\pi [b_k^\dagger b_k + \sum_+ \frac{1 - \sigma_{kl}^x}{2}] \right),$$

and $\langle b_k^\dagger b_k \rangle = N_0$.

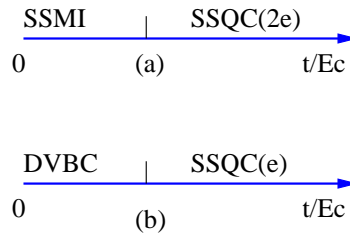


FIG. 9. States present in one-dimensional lattices with an even or odd number of spin-one bosons per site as the hopping t is varied. a) is for an even number of bosons per site; b) is for an odd number of bosons per site. DVBC states in one-dimensional Mott states are suggested by the quantum dimer model in section VIII; in the limit $t \ll \sqrt{E_s E_c}$, these states are also suggested by the bilinear-biquadratic $S = 1$ spin chain model. We believe these states appear in cold atoms in an optical lattice when laser intensities are varied. Note that SSQCs have only quasi-long range order in one-dimensional limit and charge-e or -2e character might only be distinct close to the critical points.

Therefore, the physics of spin-one bosons with anti-ferromagnetic interactions in one-dimensional lattices is effectively equivalent to the physics of spinless bosons interacting with each other via Ising gauge fields. This is the key idea behind the notion of quantum condensates of spin-one atoms; in this limit, spin-one atoms behave as if they lost their identities as spinful particles.

Let us start with an even number of particles per site. In this case, the only fixed point of the Ising gauge

field theory (unfrustrated) in one-dimensional lattices is a strong coupling fixed point regardless the value of Γ_b . The ground state for Ising fields should be unique with $\hat{T}_y = 1$ and for any link kl ,

$$\sigma_{kl}^x = 1. \quad (104)$$

And all excitations of Ising fields are fully gapped. The effective Hamiltonian can be reduced to \mathcal{H}_{pb} in Eq.73, i.e.,

$$\begin{aligned} \mathcal{H}_{pb}^{1d} &= -\tilde{t}_2 \sum_{\langle kl \rangle} (b_k^\dagger b_k^\dagger b_l b_l + h.c.) + \sum_k \frac{\rho_k^2}{2C} - \mu \rho_k, \\ (\hat{C}_k^b)^{-1} \mathcal{H}_{pb} \hat{C}_k^b &= \mathcal{H}_{pb}; \end{aligned} \quad (105)$$

Therefore when $t_2 < E_c$, the ground state is a spin singlet Mott state, or an SSMI; furthermore, we believe that when $t_2 > E_c$, chargons are paired and "condense" forming a **charge-2e** SSQC. This leads to a phase diagram for one-dimensional optical lattices in Fig.9 a).

For an odd number of particles per site and when $E_c \gg E_s$, one can carry out similar discussions. Following discussions in section VIII A and B, we find that the ground state for Ising fields has a two-fold degeneracy with $\hat{T}_y = \pm 1$, and for any link kl

$$\text{i) } \sigma_{kl}^x = (-1)^k, \text{ or } \text{ii) } \sigma_{kl}^x = (-1)^{k+1} \quad (106)$$

corresponding to two states breaking the crystal translational symmetry. And excitations are gapped. In addition, because of the Berry's phase term (see discussions in section III), the Ising fields are weakly interacting in this case.

Hopping of a chargon in this gauge field background is similar to hopping of an atom in the projected spin singlet Hilbert space. A chargon hops from site k to site $k+2$ via a virtual excitation involving an energy of E_s . More specifically, in the representation introduced in section V

$$|\dots \rho_k, d_{k,k+1}, \rho_{k+1}, d_{k+1,k+2}, \rho_{k+3}, d_{k+3,k+4} \dots\rangle$$

one confirms that the hopping corresponds to the following process

$$\begin{aligned} |\dots 2n+2, 0, 2n+1, 1, 2n+1, 0 \dots\rangle &\rightarrow \\ |\dots 2n+1, 1, 2n+2, 1, 2n+1, 0 \dots\rangle &\rightarrow \\ |\dots 2n+1, 1, 2n+1, 0, 2n+2, 0 \dots\rangle. \end{aligned}$$

Consequently, the effective Hamiltonian should be, instead of a paired hopping form

$$\mathcal{H}_{fqb}^{1d} = -\tilde{t}_2 \sum_k (b_k^\dagger b_{k+2} + h.c.) + \sum_k \frac{\rho_k^2}{2C} - \mu \rho_k. \quad (107)$$

At $G_c > G_{cc}$, chargons condense and the ground state is a **charge-e** SSQC, similar to condensates of charged solitons proposed for non-integer numbers of atoms per site [19]. Subject to strong one-dimensional fluctuations, SSQCs should be understood as states with quasi long-range phase order instead of condensates.

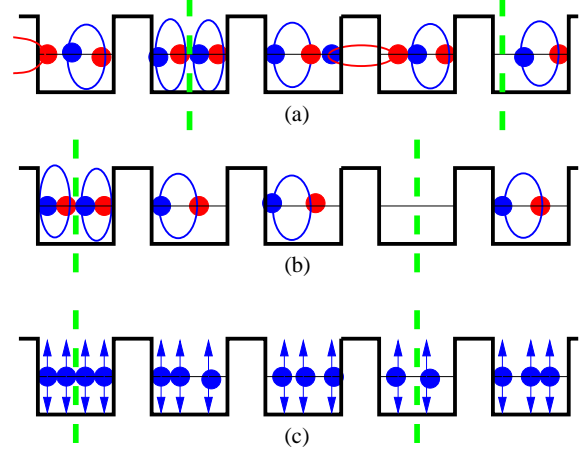


FIG. 10. Condensation of particle-hole pairs suggested by solutions to Eq.103. For an odd number of particles per site in a), a pair of particles with $\pm e$ charges are shown to condense; in b) for an even number of particles per site, a pair of particles with $\pm 2e$ charges condense. Note that these condensates are spin singlet states. As a reference, in c) we also show condensation of particle-hole pairs in a pBEC which is a stable phase only in high dimensional lattices. Locations of charges are indicated by dashed lines.

The difference between condensates for odd and even numbers of atoms per site can be attributed to the selection rule in low energy Hilbert spaces for each individual site defined in Eq.11. In one-dimensional lattices, the selection rule defined in section II leads to a two-fold degenerate DVBC for an odd number of atoms per site and a non-degenerate SSMI for an even number of atoms per site in the strong coupling limit. Therefore, elementary charged excitations are either charge-e ones or charge-2e ones depending on the parity of numbers of atoms per site in one-dimensional lattices (see also Fig.4). Consequently, condensates indicated in the fractionalized representation involve condensation of chargons or chargon-pairs depending on the parity of N_0 .

X. POSSIBLE BERRY'S PHASE EFFECTS ON SSQCS IN ONE DIMENSIONAL LATTICES

The action for Hamiltonian \mathcal{H}_{fqb}^{1d} under the constraint defined after Eq.100 can be derived following a standard procedure; the result is

$$\begin{aligned}
S = & - \sum_{\langle kl \rangle} J_{k,l} \sigma_{kl}^z \cos(\chi_k - \chi_l) \\
& - k_\tau \sum_{\square} \prod_{\square} \sigma_{kl}^z + i N_0 \frac{\pi}{2} \sum_k (1 - \sigma_{kk+\hat{e}}^z).
\end{aligned} \tag{108}$$

$J_{k,l}$ is given by

$$J_{k,k+x} = (\epsilon t), J_{k,k+\tau} = (\epsilon E_c)^{-1} \tag{109}$$

and k_τ is given in Eq.81. This action should be used to study long wave length physics in one-dimensional lattices for an arbitrary hopping amplitude.

When $J_{k,l}$ is small, the phases χ_k are disordered; these disordered phases represent Mott insulating states in one dimensional lattices which have been studied in details in section VIII. From a point of view of the action in Eq.108, differences between an even and odd number of atoms per site are only manifested in Berry's phase terms. The interesting "even-odd" effect in one-dimensional Mott states of spin-one bosons represents a well-known Berry's phase effect on spin liquids.

Results in the previous section appear to imply that properties of "Higgs" phases close to critical points should also be solely determined by the even-odd parity of numbers of atoms per site. Especially, for $N_0 = 2n$, the ordered phase represents a charge-2e SSQC and for $N_0 = 2n + 1$, the ordered phase represents a charge-e SSQC. Whether an one-dimensional lattice with cold atoms perhaps is one of few systems where the Berry phase determines how the $U(1)$ symmetry is broken spontaneously remains to be understood. In a separate paper, we are going to numerically study SSQCs and the speculated effect of Berry's phases on spontaneous symmetry breaking.

XI. CONCLUSIONS

In this article, we have illustrated the notion of fractionalized atoms and demonstrated the possibility of having SSQCs of sodium atoms in one-dimensional optical lattices. Three major arguments have been developed to investigate spin singlet Mott states and condensates. These are:

- i) In a projected spin singlet Hilbert space, spin-one bosons with antiferromagnetic interactions are equivalent to spinless bosons interacting with Ising gauge fields.
- ii) Spin singlet Mott states are fully characterized by even- and odd-class quantum dimer models.
- iii) Because of a selection rule in the Hilbert space, in one-dimensional lattices, superfluid phases of atoms can have either charge-e or charge-2e characters depending on the parity of numbers of bosons per lattice site.

It is worth emphasizing that **charge-e** and **charge-2e** condensates can be distinguished by studying frequencies in the ac Josephson effects. Finally, the even-odd parity effect discussed here also appears to be attributed to Berry's phase effects on spontaneous symmetry breaking.

Finally, we would like to mention two open questions which we believe deserve further investigation. First, the nature of states for non-integer numbers of particles per site is not clear to us; possibilities of having spin singlet condensates in certain limits in this case exist but need to be clarified. There are also issues connected with phase separation, similar to what happens in doped antiferromagnets [62,63]. Second, it is appealing to verify results proposed in this article in the context of Luttinger-liquid theories; at the moment we are not aware of such attempts and do not know if results discussed in this paper can be rederived in a Luttinger-liquid theory based approach. Although it is not clear to us whether the phenomena discussed in this article are related to the Luttinger-liquid physics, attempts along this line of thought might shed light on the further understanding of one-dimensional phases of spin-one bosons with antiferromagnetic interactions.

XII. ACKNOWLEDGEMENT

We would like to thank the Lorentz center, Leiden for its hospitality during the 2002 workshop on "quantum spin collective phenomena in solid state physics"; FZ also wants to thank the Aspen center for physics during the 2003 workshop on "quantum gases" where this work was finished. Finally, one of us (FZ) wishes to thank P. W. Anderson for his interest on this subject, F. D. M. Haldane and P. B. Wiegmann for many stimulating discussions on SSQCs. This work is supported by the Foundation FOM, the Netherlands under contracts 00CCSPP10, 02SIC25 and NWO-MK "projectruimte" 00PR1929; MS was also partially supported by a grant from Utrecht university.

APPENDIX A: CHARGE-2E EXCITATIONS IN DVBCS IN SQUARE LATTICES

For a DVBC in square lattices, the wave function can also be represented by Eq.43; the product is however carried over all even (odd) links in each row or in each column. The ground state thus has a fourfold degeneracy [19].

The excitations in 2d DVBC states have some fascinating properties. It is convenient to employ the following modified creation and annihilation operators of valence bonds,

$$\tilde{\phi}_\eta^\dagger = \phi_\eta^\dagger \bar{\delta}(\eta), \tilde{\phi}_\eta = \phi_\eta \delta(\eta). \quad (\text{A1})$$

where $\phi_\eta^\dagger, \phi_\eta$ are the creation and annihilation operators of spin singlet states of two coupled condensates defined in Eq.86 at a link η and

$$\delta(\eta) = \begin{cases} 1, & \text{if } \phi_\eta^\dagger \phi_\eta \Psi = \Psi; \\ 0, & \text{otherwise} \end{cases} \quad (\text{A2})$$

Finally, $\bar{\delta}(\eta) = 1 - \delta(\eta)$. The reduced Hamiltonian can be written as

$$\mathcal{H}_{rd} = \sum_{\eta_1, \eta_2} [V \tilde{\phi}_{\eta_1}^\dagger \tilde{\phi}_{\eta_1} \tilde{\phi}_{\eta_2}^\dagger \tilde{\phi}_{\eta_2} - T (\tilde{\phi}_{\eta_1}^\dagger \tilde{\phi}_{\eta_2}^\dagger \tilde{\phi}_{\bar{\eta}_1} \tilde{\phi}_{\bar{\eta}_2} + h.c.)] \quad (\text{A3})$$

η_1, η_2 are a pair of two parallel *adjacent* links, perpendicular to another pair $\bar{\eta}_1, \bar{\eta}_2$ in an elementary plaquette.

To facilitate discussions, we introduce a local gauge transformation \hat{E}_k at site $k = (m, n)$;

$$\hat{E}_k = \exp \left(i\pi \left[\sum_{\eta} \tilde{\phi}_\eta^\dagger \tilde{\phi}_\eta - 1 \right] \right) \quad (\text{A4})$$

where the sum is again over all neighboring sites of site k . It is easy to confirm that all the resonating valence bond configurations and the Hamiltonian are invariant under this local gauge transformation

$$\hat{E}_k \Psi = \Psi, \hat{E}_k^{-1} \mathcal{H}_{rd} \hat{E}_k = \mathcal{H}_{rd}. \quad (\text{A5})$$

To facilitate discussions, we consider a limit where two parallel valence bonds attract each other strongly and $-V$ is much greater than the exchange interaction T . (The following discussions are also expected to be valid as far as $-V < T$ because a bare $-V$ is always renormalized to infinity in this limit.) By making an expansion over $T/|V|$, one anticipates the following ground state wave function,

$$|G_1^o\rangle = |CS_1\rangle + \sum_M \left(\frac{\mathcal{V}}{V} \right)^M |CS_1\rangle$$

$$\mathcal{V} = -T \sum_{\eta_1, \eta_2} \tilde{\phi}_{\eta_1}^\dagger \tilde{\phi}_{\eta_2}^\dagger \tilde{\phi}_{\bar{\eta}_1} \tilde{\phi}_{\bar{\eta}_2} + h.c. \quad (\text{A6})$$

where $|CS_1\rangle$ is one of the four fold degenerate column states (see discussions at the beginning of this section).

Let us start with solitonic spin-one excitations. Such a spin-one excitation is created by breaking one valence bond and sending one of the unpaired condensates to infinity while keeping the other one fixed. The many-body wave function of a solitonic excitation localized at site k would thus be created by the operator

$$\Psi_{\mathcal{M}}^{S+}(k) = \mathcal{P}_{G.G.}^1 \mathbf{h}_{k,\alpha}^\dagger \prod_{\eta_e \in \mathcal{M}} \tilde{\phi}_{\eta_e}^\dagger \prod_{\eta_o \in \mathcal{M}} \tilde{\phi}_{\eta_o} \quad (\text{A7})$$

where \mathbf{h}_k^\dagger is a creation operator defined at site k . \mathcal{M} is a path starting at site k and terminated at infinity and $\eta_{o,e}$ are the odd and even links along the path (counted from site k). In one-dimensional lattices, this precisely creates a spin-one kink as shown in [19].

In a leading order of $T/|V|$, we estimate the energy of the spin-one excitation

$$E = \frac{\langle G_1^o | \Psi_{\mathcal{M}} \mathcal{H}_{rd} \Psi_{\mathcal{M}}^\dagger | G_1^o \rangle}{\langle G_1^o | \Psi_{\mathcal{M}} \Psi_{\mathcal{M}}^\dagger | G_1^o \rangle} = V L_{\mathcal{M}} \quad (\text{A8})$$

where $L_{\mathcal{M}}$ scales as the size of the system and the excitation is infinitely massive in a thermodynamical limit.

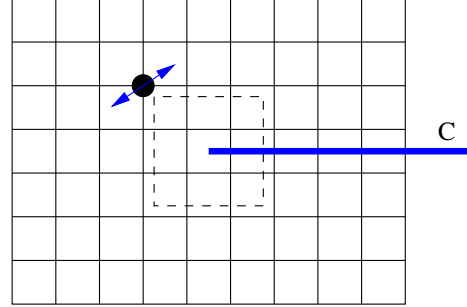


FIG. 11. Moving an $S = 1, Q = 0$ excitation (a dot with a double headed arrow) around a dual particle (defined along path \mathcal{C} , see Eq. A11) results in a minus sign in the many-body wave function; a dual particle and an $S = 1, Q = 0$ excitation view each other as half vortices.

The absence of spin-one solitonic excitations in the low energy excitation spectra doesn't depend on the particular form of wave functions we used. It is a topological property of the ground state which determines the interactions between solitonic excitations. Here we are going to provide some understanding based on the duality between spin excitations which are "electric" and topological excitations with dual "magnetic" charges.

To identify this gauge transformation \hat{E}_k as the one of Ising gauge fields, one notices typically

$$\hat{E}_k^{-1} \tilde{\Sigma}_\eta^z \hat{E}_k = (-1)^{\pi(\eta,k)} \tilde{\Sigma}_\eta^z, \tilde{\Sigma}_\eta^z = \tilde{\phi}_\eta^\dagger - \tilde{\phi}_\eta. \quad (\text{A9})$$

Here $\pi(\eta, k)$ is unity if link η is connected with site k ; otherwise it is zero. As $\tilde{\Sigma}^z$ satisfies the algebras of Pauli matrices and should be identified as σ^z of the Ising gauge fields, the local gauge transformation effectively yields $\sigma^z \rightarrow -\sigma^z$ and generates a desired Ising gauge transformation.

An operator carries an "electric" charge if it transforms nontrivially under the local gauge transformation. In our case, we can show that

$$\hat{E}_k^{-1} \Psi_{\mathcal{M}}^{S+}(k') \hat{E}_k = (-1)^{\delta(k-k')} \Psi_{\mathcal{M}}^{S+}(k'); \quad (\text{A10})$$

and the creation operator of a spin one solitonic excitation carries a charge defined with respect to the local

gauge transformation. The corresponding particle thus is topological in nature and violates the invariance defined in Eq.A5 only at the site k' where the particle is created.

Furthermore, we can introduce a creation operator of a dual magnetic charge;

$$\Psi_{\mathcal{C}}^{e+}(x, y) = \prod_{\eta \in \mathcal{C}} (2\tilde{\phi}_{\eta}^{\dagger} \tilde{\phi}_{\eta} - 1) \quad (\text{A11})$$

where the path \mathcal{C} begins at the center of a plaquette (x, y) and ends at infinity by piercing all links intersecting with it. In the leading order of $T/|V|$, one also finds that

$$\Psi_{\mathcal{C}}^{e+}|G_1^o\rangle \approx (-1)^{N_{\mathcal{M}}}|G_1^o\rangle \quad (\text{A12})$$

where $N_{\mathcal{M}}$ is the number of unoccupied links along the path \mathcal{M} . This implies that the ground state should be a condensate of dual particles.

Now one can move a spin-one solitonic spin excitation $\Psi_{\mathcal{M}}^{\dagger}$ around a dual magnetic charge $\Psi_{\mathcal{C}}^{\dagger}$. In the Hilbert space spanned by valence bond configurations, the following commutation relation holds:

$$\{(2\tilde{\phi}_{\eta}^{\dagger} \tilde{\phi}_{\eta} - 1), \tilde{\phi}_{\eta}^{\dagger}\} = \{(2\tilde{\phi}_{\eta}^{\dagger} \tilde{\phi}_{\eta} - 1), \tilde{\phi}_{\eta}\} = 0. \quad (\text{A13})$$

Following Eq. A13, one verifies that the many-body wave function changes sign after this operation (shown in FIG.11). This implies remarkable long range correlations in the system. Since the "magnetic" and "electric" charges in the theory see each other as half-flux-quanta, it is imaginable that as one of the charges condenses, the other one gets confined following a standard picture in topological field theories. In the current context, the dual magnetic charges condense and spin-one solitonic spin excitations are confined because of random phases developed when moving in a dual magnetic charge condensate.

We are now ready to address the quantum numbers of *elementary* spin excitations. Because of confining forces between $S = 1$ solitonic excitations, only bound states of soliton-anti soliton pairs can exist in the excitation spectrum as elementary excitations. So there will be two branches spin excitations with $S = 1$ and $S = 2$ respectively. Taking into account Eq.33, we should further expect the bound states of $S = 2$ have lower energies than $S = 1$. In fact, microscopically these bound states are likely to be the excited states of $S = 2$ and $S = 1$ of two coupled neighboring condensates.

A **charge-e** soliton can be created by adding an atom to a site while keeping the rest of sites paired; this excitation is a spin singlet as the ground state but with an extra atom or **charge-e**. For the same reason discussed before for a spin-one solitonic excitation, a charged soliton is infinitely massive because of the long range rearrangement of valence bonds and intends to pair with another charged soliton. Naturally, at low energies, one can only have **charge-2e** spin singlet excitations in this case.

APPENDIX B: THE DERIVATION OF THE FRACTIONALIZED REPRESENTATION

The equivalence between Eq. 6 and Eq.56 can be demonstrated by examining the partition function,

$$\mathcal{Z} = \text{Tr}[\exp(-\beta\mathcal{H}_{FR})\mathcal{P}]; \quad (\text{B1})$$

\mathcal{P} is a projection operator defined in Eq.(B6)

To facilitate the calculation, we introduce the following special "coherent" state representation

$$\begin{aligned} |\mathbf{n}\rangle &= \frac{1}{\sqrt{2\delta N}} \sum_{N_0-\delta N}^{N_0+\delta N} \frac{(\mathbf{n} \cdot \mathbf{a}^{\dagger})^n}{\sqrt{2(n-1)!}} |0\rangle, \\ |z\rangle &= \frac{1}{\sqrt{2\delta N}} \sum_{N_0-\delta N}^{N_0+\delta N} \frac{(zb^{\dagger})^n}{\sqrt{2(n-1)!}} |0\rangle \end{aligned} \quad (\text{B2})$$

assuming that $N_0 \gg \delta N$ but both are much larger than unity and $z = \exp(i\phi)$. One can easily show that at large N limit,

$$\langle \mathbf{n}|\mathbf{n}'\rangle \approx \delta(\mathbf{n} - \mathbf{n}'), \langle z|z'\rangle \approx \delta(z - z'); \quad (\text{B3})$$

and

$$\begin{aligned} \rho|z\rangle &= \frac{\partial}{\partial \ln z}|z\rangle \\ \mathbf{S}|\mathbf{n}\rangle &= i\mathbf{n} \times \frac{\partial}{\partial \mathbf{n}}|\mathbf{n}\rangle. \end{aligned} \quad (\text{B4})$$

For the study of the action, we slice the $(d+1)$ dimensional Euclidean space into M slices along the temporal direction and rewrite the partition function as

$$\begin{aligned} \mathcal{Z} &= \prod_{\tau} \langle \{\mathbf{n}_{k,\tau}\}, \{z_{k,\tau}\}, \{\sigma_{k,\tau}^z\} | \exp(-\epsilon\mathcal{H}_{FR})\mathcal{P} \\ &| \{\mathbf{n}_{k,\tau+\epsilon}\}, \{z_{k,\tau+\epsilon}\}, \{\sigma_{k,\tau+\epsilon}^z\} \rangle. \end{aligned} \quad (\text{B5})$$

Here τ and $\tau + \epsilon$ label two adjacent slices and $\epsilon = \beta/M$. The projection operator is to impose a constraint due to the symmetry of many-boson wave functions,

$$\mathcal{P} = \sum_{\xi_k=\pm 1} \exp[i\frac{1+\xi_k}{2}\pi(n_k + S_k)] \quad (\text{B6})$$

so that only states with an even $n_k + S_k$ contribute to the functional integral.

The matrix element in Eq.B5 can be conveniently evaluated by inserting a complete set of n_k, S_k , the eigen states of the number and spin operators.

$$\begin{aligned} &\sum_{\{n_k\}, \{S_k\}} \langle \{\mathbf{n}_{k,\tau}\}, \{z_{k,\tau}\}, \{\sigma_{k,\tau}^z\} | \exp(-\epsilon\mathcal{H}_{FR})\mathcal{P} \otimes \\ &| \{n_k\}, \{S_k\} \rangle \langle \{n_k\}, \{S_k\} | \{ \mathbf{n}_{k,\tau+\epsilon} \}, \{z_{k,\tau+\epsilon}\}, \{\sigma_{k,\tau+\epsilon}^z\} \rangle. \end{aligned} \quad (\text{B7})$$

Here $z_k = \exp(i\chi_k)$.

Consider a simplified situation of a planar $\mathbf{n} = (\cos \phi, \sin \phi, 0)$ (a generalization appears to be possible). As suggested in Eq.B4, \mathbf{S} and ρ are conjugate variables of \mathbf{n} and ϕ . So we can express the eigen states $|n_k\rangle$, $|l_k\rangle$ in the following simple forms

$$\begin{aligned}\langle z_k | n_k \rangle &= \frac{1}{\sqrt{2\pi}} \exp(i\chi_k n_k), \\ \langle \mathbf{n}_k | S_k \rangle &= \frac{1}{\sqrt{2\pi}} \exp(i\phi_k S_k).\end{aligned}\quad (\text{B8})$$

The rest of the derivation is identical to that in [11]. Redefining ξ_k as σ^z along a link located at site k between slice τ and $\tau + \epsilon$ and summing up all contributions at different slices, we obtain the result in the Euclidean space as

$$\begin{aligned}S &= - \sum_{rr'} J_{rr'}^c \sigma_{rr'}^z \cos \chi_{rr'} - \sum_{rr'} J_{rr'}^{2c} \cos(2\chi_{rr'}) \\ &\quad - \sum_{rr'} J_{rr'}^s \sigma_{rr'}^z \mathbf{n}_r \cdot \mathbf{n}_{r'} - \sum_{rr'} J_{rr'}^{2s} Q_r^{ab} Q_{r'}^{ab} \\ &\quad + iN_0 \sum_r \frac{1 - \sigma_{rr}^z}{2} \pi\end{aligned}\quad (\text{B9})$$

Here summation goes over sites $r = (k, \tau)$ in the space-time lattice, $\chi_{rr'} = \chi_r - \chi_{r'}$, and

$$Q_r^{ab} = \mathbf{n}_r^a \mathbf{n}_r^b - \delta^{ab}/3$$

is a nematic order parameter, and $\sigma_{rr'}^z = \pm 1$ is an Ising field that lives on the links and $r_\tau = r + \hat{e}$.

The coupling constants are

$$\begin{aligned}J_{r,r\pm\hat{\tau}}^c &= \frac{1}{E_c \epsilon}, J_{r,r\pm\hat{\tau}}^s = \frac{1}{E_s \epsilon}, J_{r,r\pm\{\hat{x},\hat{y},\hat{z}\}}^{c,s} = \epsilon t N_0, \\ J_{r,r\pm\hat{\tau}}^{2c} &= J_{r,r\pm\hat{\tau}}^{2s} = 0, J_{r,r\pm\{\hat{x},\hat{y},\hat{z}\}}^{2c,2s} = -\epsilon t N_0/4\end{aligned}$$

This is precisely the action of Eq. 1 derived in an early work [11] (the Berry's phase term was omitted there). Therefore we established an anticipated equivalence between Eq. 1 and Eq.56. Finally, we would like to mention that Ising-gauge-theory based approaches have also been employed to study electron fractionalization in previous works [28–31,33,47–49].

APPENDIX C: NMIS IN HIGH DIMENSIONAL LATTICES: REVISIT I

As chargons are fully gapped, states in this limit are incompressible. Integrating out chargons' or b -particles' degree of freedom in Eq.62 we end up with an effective Hamiltonian

$$\begin{aligned}\mathcal{H}_{fqca} &= -\tilde{t} \sum_{\langle kl \rangle} (\mathbf{a}_{k\alpha}^\dagger \mathbf{a}_{l\alpha} \sigma_{kl}^z + h.c.) + \sum_k \frac{\mathbf{S}_k^2}{2I} \\ &\quad + \Gamma_a \sum_{\langle kl \rangle} \sigma_{kl}^x - K_{sa} \sum_{\square} \prod_{\square} \sigma_{kl}^z.\end{aligned}\quad (\text{C1})$$

Calculations indicate that Γ_a, K_{sa} should be functions of t, E_c . When t is much smaller than E_c , or $G_c = tE_c^{-1}$ is small, the ratio $K_{sa}\Gamma_a^{-1}$ is much less than unity, or

$$\frac{K_{sa}}{\Gamma_a} \ll 1 (\Gamma_a \sim E_c). \quad (\text{C2})$$

However, we speculate that close to the critical value G_{cc} , the ratio in Eq. C2 should be divergent (one should also expect terms involving large loops). Finally, the integration also leads to a new constraint on the Hilbert space,

$$\hat{C}_k^{fa} \Psi = \Psi, \hat{C}_k^{fa} = \exp \left(i\pi [\mathbf{a}_k^\dagger \mathbf{a}_k + \sum_{+} \frac{1 - \sigma_{kl}^x}{2}] \right). \quad (\text{C3})$$

The sum over "+" is again carried over all links connected to site k . And the Hamiltonian is locally invariant under the action of \hat{C}_k^{fa}

$$(\hat{C}_k^{fa})^{-1} \mathcal{H}_{fqca} \hat{C}_k^{fa} = \mathcal{H}_{fqca}. \quad (\text{C4})$$

The condensation can be easily visualized when t is close to $E_c G_{cc}$, or in the large K_{sa} limit. The gauge fields are weakly interacting and fluctuations are small. For instance, one can estimate the probability of finding a loop of plaquettes with $\prod_{\square} \sigma_{kl}^z = -1$ in $(2+1)$ Euclidean space is exponentially small.

It is therefore tempting to work out a self-consistent solution in a "mean field" approximation where $\prod_{\square} \sigma_{kl}^z = 1$ at each plaquette. Furthermore, one chooses a unity gauge

$$\sigma_{kl}^z = 1, \text{ for any link.} \quad (\text{C5})$$

One then obtains a FQCa, or an \mathbf{a} -type FQC, as the ground state in this case. In FQCa,

$$\mathcal{G}^b(k, k + \infty) = 0, \mathcal{G}_{\alpha\beta}^{\mathbf{a}}(k, k + \infty) \sim \mathbf{n}_\alpha \mathbf{n}_\beta \quad (\text{C6})$$

as spin-one spinons condense in a state created by an operator $\mathbf{a}_{Q=0}^\dagger \cdot \mathbf{n}$.

It is also possible to show the existence of the fractionalized phase beyond this simple mean field theory. In a dilute gas approximation suggested in [57], one finds an up-bound of the correction to $\mathcal{G}_{\alpha\beta}^{\mathbf{a}}(k, k + \infty)$ calculated in a mean field approximation which is exponentially small as K_{sa} or G_s is large. One therefore expects that the conclusions arrived above are valid beyond the mean field approximation.

The ground state of FQCa does not exhibit phase coherence or Josephson effects. However, the rotational symmetry is broken. There are two branches gapless spin wave excitations (spin one); the zeroth sound involving

the compression or expansion of particle-densities is fully gapped.

A more tricky situation is when t is much less than E_c or correspondingly when Γ_a is large and gauge fluctuations are strong in the absence of matter fields. To argue the existence of condensation in this case, one recalls that there are no phase transitions when K_a is varied but G_s is kept at infinity. Physically, presence of matters strongly renormalizes gauge field dynamics. A condensate represents a self-consistent solution to the problem provided t is much larger than E_s ; this conventional point of view is supported by results in [64]. However, since pure gauge fields at large Γ_a limit are confining, only pairs of $\mathbf{a}^\dagger \mathbf{a}^\dagger$ are free excitations at small t limit; as t is increased, condensation appears to only involve these pairs [65,66]. To illustrate this point, we present some detailed discussions on pFQCa.

As stated at the beginning of this section, there are even numbers of atoms at each site. Consequently, each site is occupied by an even number of chargons; excitations involving a change of numbers of chargons at each site are gapped by an energy of order of E_c . At energies much lower than E_c , the constraint in Eq.55 then indicates that the low energy Hilbert space should be spanned by states satisfying

$$\hat{C}_k^a \Psi = \Psi, \hat{C}_k^a = \exp(i\pi \mathbf{a}_k^\dagger \cdot \mathbf{a}_k). \quad (\text{C7})$$

In this subspace defined by two-particle operators $(\mathbf{a}_k^\dagger)^2$, the relevant Hamiltonian is due to pair hopping following Eqs.56,62,

$$\begin{aligned} \mathcal{H}_{pa} &= -\tilde{t}_1 \sum_{\langle kl \rangle} (\mathbf{a}_{k\alpha}^\dagger \mathbf{a}_{k\beta}^\dagger \mathbf{a}_{l\alpha} \mathbf{a}_{l\beta} + h.c.) + \sum \frac{\mathbf{S}_k^2}{2I} \\ (\hat{C}_k^a)^{-1} \mathcal{H}_{pa} \hat{C}_k^a &= \mathcal{H}_{pa}. \end{aligned} \quad (\text{C8})$$

and

$$\tilde{t}_1 \approx \frac{t^2}{\Gamma_a} (\Gamma_a \sim E_c). \quad (\text{C9})$$

By examining the Hamiltonian in this reduced space, assuming $t_1 = \tilde{t}_1 N_a^2 \gg E_s$, one concludes that the ground state is a condensate of paired spinons, or pFQCa. In a lattice with V_T sites, the wave function of a pFQCa can be written as (up to a normalization factor)

$$\begin{aligned} |g_1\rangle &= \prod_k \frac{b_k^{+2n}}{\sqrt{2n!}} \otimes \mathcal{P}_{N_a \times V_T} \exp(\Phi_a^\dagger(Q_0 = 0)) |0\rangle. \\ \Phi_a^\dagger(Q_0) &= \mathbf{Q}_{\alpha\beta} \sum_q \mathbf{a}_{q,\alpha}^\dagger \mathbf{a}_{-q+Q_0,\beta}^\dagger \end{aligned} \quad (\text{C10})$$

which explicitly satisfies the above constraint. Here $\Psi_a^\dagger(Q_0)$ is a creation operator for a pair of spinons in $(Q_0 - q, q)$ channel. The sum over q is carried over the first Brillouin zone. $\mathcal{P}_{N_a \times V_T}$ is to project out $N_a \times V_T$ -particle states.

In a pFQCa, $\mathcal{G}_{\alpha\beta}^{\mathbf{a}}(k, l)$ and $\mathcal{G}^b(k, l)$ vanish as $k - l$ approaches infinity. However, the rotational symmetry is still broken and there exists the following long range order in the generalized BCS wave function

$$\Delta_{\alpha\beta}^{\mathbf{a}}(k, k) = 3\mathbf{Q}_{\alpha\beta} \quad (\text{C11})$$

which is invariant under the local gauge transformation defined in Eq.58.

The difference between pFQCa and FQCa is subtle. Both of them break rotational symmetry, support gapless modes and have similar local dynamics. On the other hand, topological excitations in two states are distinct.

Let us also mention briefly that when $E_s \gg t, t_1$, only localized singlet pairs of spinons are allowed in the system. These states can be identified as SSIMs discussed in section II.

APPENDIX D: DVBC'S IN A FRACTIONALIZED REPRESENTATION

As shown in some details, the ground state for an odd N_0 when $G_{s,t} \ll 1$ is a projected superposition of paired condensates in $(q, -q)$ and $(q, \pi - q)$ channels and has a two-fold degeneracy. The corresponding wave functions of the two-fold degenerate ground states are topologically identical to

$$\begin{aligned} |g_3\rangle &= \prod_k (b_k^\dagger)^{2n+1} \otimes \frac{(\mathbf{a}_{k\alpha}^\dagger \mathbf{a}_{k\alpha}^\dagger)^n}{\sqrt{(2n+1)!}} \\ \mathcal{P}_{G.G.}^1 \exp[\sum_{\gamma=0,1} g_\gamma \Phi_{as}^\dagger(\gamma\pi)] |0\rangle; \\ \Phi_{as}^\dagger(Q_0) &= \sum_q \frac{h(q)}{2\sqrt{3}} \mathbf{a}_{Q_0+q,\beta}^\dagger \mathbf{a}_{-q,\beta}^\dagger \end{aligned} \quad (\text{D1})$$

where $h(q)$ is chosen to be $\exp(iq)$. Two fold degenerate states correspond to $g_0 = g_1 = 1$ or $g_0 = -g_1 = 1$. It is straightforward to establish an equivalence between this projected pFQCa state and dimerized valence bond crystals studied previously [19].

APPENDIX E: THE DERIVATION OF EQ.80

Let us consider a limit where χ and \mathbf{n} have short range correlations and

$$\langle \cos \chi_r \cos \chi_l \rangle = C_\chi, \langle \mathbf{n}_r \mathbf{n}_l \rangle = C_{\mathbf{n}}. \quad (\text{E1})$$

only if k, l are two neighboring sites.

Using the standard high temperature expansion technique, one integrates out \mathbf{n}, χ in the action given in Eq.B9. The results in the leading order are

$$\mathcal{Z}(\{\sigma_i^z\}) \sim \prod_i \sum_{\sigma_i^z = \pm 1} \{1 - (\epsilon t)^4 \sum_{kl, lm, mn, nk}^s \sigma_{kl}^z \sigma_{lm}^z \sigma_{mn}^z \sigma_{nk}^z\} \quad (\text{E2})$$

$$-[(\frac{t}{E_c})^2 + (\frac{t}{E_s})^2] \sum_{kl, lm, mn, nk}^\tau \sigma_{kl}^z \sigma_{lm}^z \sigma_{mn}^z \sigma_{nk}^z \} \quad (\text{E3})$$

$$\times \exp(iN_0 \sum_r \frac{1 - \sigma_{rr}^z}{2} \pi). \quad (\text{E4})$$

The sum in Eq.E2 is over all elementary spatial plaquettes occupied by links kl, lm, mn, nk ; the sum in Eq.E3 is over elementary plaquettes involved both spatial links kl, mn and temporal links lm, nk ; without losing generality, we have set C_χ and C_n to be unity. The structure of Eq.E2 is identical to Eq.80; further more, comparing Eqs.E2,E3,E4 with Eq.80, one obtains results in Eq.81.

APPENDIX F: GAUGE INVARIANT CORRELATION FUNCTIONS

It is tempting to classify SSQCs or more general FQCs in terms of local order parameters similar to those in Eq.1. To characterize FQCs, in addition one should introduce

$$\mathcal{O}^0 = \langle \psi_{k\alpha} \psi_{k\alpha} \rangle. \quad (\text{F1})$$

In terms of order parameters $\mathcal{O}^{0,1,2}$,

$$\begin{aligned} \text{pBEC: } & \mathcal{O}_\alpha^1 \neq 0, \mathcal{O}_{\alpha\beta}^2 \neq 0, \mathcal{O}^0 \neq 0; \\ \text{SSQC(2e): } & \mathcal{O}_\alpha^1 = 0, \mathcal{O}^0 \neq 0, \mathcal{O}_{\alpha\beta}^2 = 0; \\ \text{pFQCa: } & \mathcal{O}_\alpha^1 = 0, \mathcal{O}_{\alpha\beta}^2 \neq 0, \mathcal{O}^0 = 0. \end{aligned} \quad (\text{F2})$$

For FQCa and SSQC(e) states, the order parameters are nonlocal in terms of ψ^\dagger and will be introduced in a subsequent paper on fractionalized states for non-integer numbers of bosons per site.

We would like to make two more remarks on FQCs. First, Elitzur theorem claims that in the presence of local gauge invariance, operators such as $\sigma_k^\pm, \mathbf{a}_k^\dagger, b_k^\dagger$ which transform nontrivially under the local gauge transformation can not develop nonzero expectation values [67]. The existence of FQCs which so far is explicitly demonstrated in a fixed gauge at first sight appears to be at odds with the Elitzur theorem. The apparent paradox can be formally resolved if one carries out a similar calculation in terms of gauge invariant correlators and confirms long range order.

Indeed, for discussions on quantum condensates, one can also study the following gauge invariant two-point correlation functions

$$\begin{aligned} G_{\alpha\beta}^a(k, l) &= \langle \mathbf{a}_{k\alpha}^\dagger \prod_{C_{kl}} \sigma_t^z \mathbf{a}_{l\beta} \rangle \langle \prod_{C_{kl}^4} \sigma_t^z \rangle^{-1/4} \\ G^b(k, l) &= \langle b_k^\dagger \prod_{C_{kl}} \sigma_t^z b_l \rangle \langle \prod_{C_{kl}^4} \sigma_t^z \rangle^{-1/4} \end{aligned} \quad (\text{F3})$$

where the products are carried over links along path C_{kl} and C_{kl}^4 . C_{kl} is a path connecting k and l site and C_{kl}^4 is a closed path of four times as long. These correlation functions characterize the condensates when the gauge fields are weakly interacting [68].

Gauge invariant correlators suggest that it should not be bare \mathbf{a} - or b -particles but some nonlocal "particles" which condense. One such candidate is an \mathbf{a} or b -particle dressed in a string of gauge fields

$$\mathbf{A}_{k\alpha}^\dagger(C_k) = \mathbf{a}_{k\alpha}^\dagger \prod_{C_k} \sigma_\eta^z, B_k^\dagger(C_k) = b_k^\dagger \prod_{C_k} \sigma_\eta^z \quad (\text{F4})$$

where C_k is a path starting at site k and terminated at infinity. One can easily confirm the following local gauge invariance of these operators

$$\begin{aligned} (\hat{C}_k^{fa})^{-1} \mathbf{A}_{k\alpha}^\dagger \hat{C}_k^{fa} &= \mathbf{A}_{k\alpha}^\dagger, \\ (\hat{C}_k^{fb})^{-1} B_k^\dagger \hat{C}_k^{fb} &= B_k^\dagger. \end{aligned} \quad (\text{F5})$$

These particles can condense without violating the Elitzur theorem. On the other hand they carry exactly the same charge and spin as bare particles of \mathbf{a}^\dagger and b^\dagger . We speculate that condensation of \mathbf{a} or b -particles in a fixed gauge might also imply condensation of particles created by \mathbf{A}^\dagger and B^\dagger .

The second remark concerns the relation between charge-e SSQCs and previously discussed spin singlet paired condensates or charge-2e SSQCs [11]. Both condensates are rotationally invariant spin singlets and both are phase coherent. However, from the point of view of correlations it is obvious that charge-e SSQC doesn't involve pairing of particles and differs from paired condensates. An explicit construction of wave functions of charge-e SSQC is difficult but available. At the time of writing, we believe that FQCs represent condensation of some topological solitons which in short are called as \mathbf{a} -, b - particles. Particularly, charge-e SSQCs should exist in lattices with both non-integer and integer numbers of atoms per site.

-
- [1] D.M. Stamper-Kurn, M. R. Andrews, A.P. Chikkatur, S. Inouye, H.-J. Miesner, J. Stenger and W. Ketterle, Phys. Rev. Lett. **80**, 2027(1998).

- [2] J. Stenger, S. Inouye, D.M. Stamper-Kurn, H.-J. Miesner, A.P. Chikkatur and W. Ketterle, *Nature* **396**, 345(1998).
- [3] T. L. Ho, *Phys. Rev. Lett.* **81**, 742 (1998).
- [4] T. Ohmi and K. Machida, *J. Phys. Soc. Jpn.* **67**, 1822(1998).
- [5] C. K. Law et al., *Phys. Rev. Lett.* **81**, 5257(1998).
- [6] T. L. Ho and S. K. Yip, *Phys. Rev. Lett.* **84**, 4031(2000).
- [7] T. L. Ho and E. Mueller, *Phys. Rev. Lett.* **89**, 050401 (2002).
- [8] J. W. Reijnders, F. J. M. van Lankvelt, K. Schoutens and N. Read, *Phys. Rev. Lett.* **89**, 120401(2002); *cond-mat/0306402*.
- [9] M. P. Fisher, P. B. Weichman, G. Grinstein and D. S. Fisher, *Phys. Rev. B* **40**, 546-570(1989).
- [10] M. Greiner, O. Mandel, T. Esslinger, T. Hänsch and I. Bloch, *Nature* **415**, 39(2002).
- [11] E. Demler and F. Zhou, *Phys. Rev. Lett.* **88**, 163001-1(2002); E. Demler, F. Zhou and D. F. M. Haldane, *ITP-UU-01/09*(2001).
- [12] S. Yip, *cond-mat/0306018*.
- [13] S. Tsuchiya, S. Kurihara and T. Kimura, *cond-mat/0209676*.
- [14] A. Imambekov, M. Lukin and E. Demler, *cond-mat/0306204*(2003).
- [15] M. Snoek and F. Zhou, *cond-mat/0306198*(2003).
- [16] A.F. Andreev and I.A. Grischuk, *Sov. Phys. JETP* **60**(2), 267(1984) [*Zh. Eksp. Teor. Fiz.* **87**, 467 (1984)].
- [17] A.V. Chubukov, *J. Phys. Cond. Mat.* **2**, 1593 (1990).
- [18] P. Chandra, P. Coleman, and A. Larkin, *J. Phys. Cond. Mat.* **2**, 7933(1990).
- [19] Fei Zhou, *Euro. Phys. Lett.* **63**(4), 505(2003) [See also *cond-mat/0207041*].
- [20] I. Affleck, T. Kennedy, E. H. Lieb and H. Tasaki, *Phys. Rev. Lett.* **59**, 799(1987).
- [21] I. Affleck, *J. Phys: Condens. Matter* **1**, 3047 (1989).
- [22] D. P. Arovas, A. Auerbach and F. D. Haldane, *Phys. Rev. Lett.* **60**, 531(1988).
- [23] J. B. Parkinson, *J. Phys. C* **21**, 3793(1988).
- [24] M. N. Barber and M. T. Batchelor, *Phys. Rev. B* **40**, 4621 (1989).
- [25] A.V. Chubukov, *Phys. Rev. B* **43**, 3337 (1991).
- [26] F. D. M. Haldane, *Phys. Rev. Lett.* **61**, 1029(1988).
- [27] N. Read and S. Sachdev, *Phys. Rev. Lett.* **62**, 1694(1989).
- [28] N. Read and S. Sachdev, *Phys. Rev. Lett.* **66**, 1773(1991); S. Sachdev, *Phys. Rev. B* **45**, 12377(1992).
- [29] R. A. Jalabert and S. Sachdev, *Phys. Rev. B* **44**, 686(1991).
- [30] T. Senthil and M. P. Fisher, *Phys. Rev. B* **62**, 7850(2000); *Phys. Rev. Lett.* **86**, 292(2001).
- [31] T. Senthil and M. P. Fisher, *cond-mat/0008082*.
- [32] D.S. Rokhsar and S.A. Kivelson, *Phys. Rev. Lett.* **61**, 2376(1988); S. A. Kivelson, J. Senthil and D. S. Rokhsar, *Phys. Rev. B* **35**, 8865(1987).
- [33] R. Moessner, S. L. Sondhi and E. Fradkin, *Phys. Rev. B* **65**, 024504(2002).
- [34] F. Zhou, *Phys. Rev. Lett.* **87**, 080401-1(2001); F. Zhou, *Int. Jour. Mod. Phys. B* **17** No. 14, 2643-2698(2003) [also *cond-mat/0108473*].
- [35] W. Vincent Liu and X-G. Wen, *cond-mat/0201187*.
- [36] We acknowledge very useful discussions with E. Demler, and E. Fradkin in the Lorentz center in the summer 2002. Concerns from them and later on from N. Read, S. Sachdev, J. Zaanen, especially S. Z. Zhang have partially motivated us to clarify the microscopic structure of charge-e SSQCs.
- [37] P. W. Anderson, *Science* **235**, 1196(1987).
- [38] G. Baskaran and P.W. Anderson, *Phys. Rev. B* **37**, 580(1988).
- [39] G. Baskaran, Z. Zou and P. W. Anderson, *Solid State Comm.* **63**, 973(1987).
- [40] I. Affleck and J. B. Marston, *Phys. Rev. B* **37**, 3774(1988).
- [41] L. Ioffe and A. Larkin, *Phys. Rev. B* **39**, 8988(1989).
- [42] X. G. Wen, *Phys. Rev. B* **39**, 7223(1989).
- [43] X. G. Wen, F. Wilczek and A. Zee, *Phys. Rev. B* **39**, 11413(1989).
- [44] P. A. Lee, *Phys. Rev. Lett.* **63**, 680(1989).
- [45] E. Fradkin and S. Kivelson, *Mod. Phys. Lett. B* **4**, 11693(1990).
- [46] N. Read and S. Sachdev, *Phys. Rev. B* **44**, 686(1991).
- [47] X. G. Wen, *Phys. Rev. B* **44**, 2664(1991).
- [48] L. Balents, M. P. Fisher and C. Nayak, *cond-mat/9811236*.
- [49] S. Sachdev and M. Vojta, *J. Phys. Soc. Jpn.* **69**, Suppl. **B**, 1(2000).
- [50] R. Moessner and S. L. Sondhi, *Phys. Rev. Lett.* **86**, 1881(2001).
- [51] E. Demler, C. Nayak, H. Y. Kee, Y. B. Kim and T. Senthil, *Phys. Rev. B* **65**, 155103(2002).
- [52] P.W. Anderson, *The theory of superconductivity in the High-T_c cuprates*, Princeton University Press, Princeton (1997).
- [53] F. D. M. Haldane, *Phys. Rev. Lett.* **50**, 1153(1983).
- [54] A. J. Heeger, S. Kivelson, J. R. Schrieffer and W. P. Su, *Rev. Mod. Phys.* **60**, 781(1988).
- [55] F. Wegner, *J. Math. Phys.* **12**, 2259(1971);
- [56] K. G. Wilson, *Phys. Rev. B* **10**, 2445(1974).
- [57] E. Fradkin and S. Shenker, *Phys. Rev. D* **19**, 3682(1979).
- [58] J. Kogut, *Rev. Mod. Phys.* **51**, 659(1979).
- [59] The symmetry consideration does also allow additional terms such as $b_k^\dagger b_k^\dagger b_l b_l$, $\mathbf{a}_{k\alpha}^\dagger \mathbf{a}_{k\alpha}^\dagger \mathbf{a}_{l\alpha} \mathbf{a}_{l\alpha}$ in \mathcal{H}_{MG} ; we do not take into account these terms in this report.
- [60] However, this hypothesis appears to be at odds with recent numerical results on the bilinear-biquadratic model in square lattices [K. Harada and K. Kawashima, *Phys. Rev. B* **65**, 052403 (2002)]. So strictly speaking, discussions on square lattices might be valid only when extra frustration is present so that ground states are quantum disordered. The mechanism which results in quantum disordered phase is beyond the scope of this work.
- [61] D. F.M. Haldane pointed out to one of us (FZ) that some spiral spin states can also be characterized by Z_2 gauge fields; destructive interferences between instantons were discussed in his unpublished work.
- [62] J. Zaanen and O. Gunnarsson, *Phys. Rev. B* **40**, 7391(1989).
- [63] H. J. Schultz, *Phys. Rev. Lett.* **64**, 1445(1990).
- [64] P. E. Lammert, D. S. Rokhsar and J. Toner, *Phys. Rev. Lett.* **70**, 1650(1993).
- [65] However, it is not clear how phase transitions between pFQCa and FQCa states take place.

- [66] For discussions on $o(2) \times Z_2$ model, see R. D. Sedgewick, D. J. Scalapino, and R. L. Sugar, cond-mat/0012028.
- [67] S. Elitzur, Phys. Rev. **D 12**, 3978(1975).
- [68] We thank J. Smit for pointing out to us the gauge invariant two point correlation functions.